Calhoun: The NPS Institutional Archive

DSpace Repository

Theses and Dissertations | 1. Thesis and Dissertation Collection, all items

1951

Energy levels in A [Superscript 38] and Ti [Superscript 46] from the p,n reaction on C1 [Superscript 37] and Sc [Superscript 45] respectively

Schoenfeld, William August; Duborg, Robert Wayne

Massachusetts Institute of Technology

http://hdl.handle.net/10945/14148

Downloaded from NPS Archive: Calhoun

Calhoun is the Naval Postgraduate School's public access digital repository for research materials and institutional publications created by the NPS community. Calhoun is named for Professor of Mathematics Guy K. Calhoun, NPS's first appointed -- and published -- scholarly author.

Dudley Knox Library / Naval Postgraduate School
411 Dyer Road / 1 University Circle
Monterey, California USA 93943

http://www.nps.edu/library

ENERGY LEVELS IN A^{38}
AND Ti^{46} FROM THE p,n
REACTION ON Cl^{37} and Sc^{45}
RESPECTIVELY

by

LCDR. William August Schoenfeld
and
LCDR. Robert Wayne Duborg
Course VIII

OX3 - MIT

THESIS
S34

ENERGY LEVELS IN A^{38} AND Ti^{46} FROM THE p,n REACTION ON Cl^{37} AND Sc^{45} RESPECTIVELY

by

Lieutenant Commander WILLIAM AUGUST SCHOENFELD

B.S., U.S. Naval Academy
(1941)

and

Lieutenant Commander ROBERT WAYNE DUBORG

B.S., U.S. Naval Academy
(1942)

SUBMITTED IN PARTIAL FULFILLMENT OF THE
REQUIREMENTS FOR THE DEGREE OF
MASTER OF SCIENCE IN PHYSICS

at the

MASSACHUSETTS INSTITUTE OF TECHNOLOGY
(1951)

ENERGY LEVELS IN A^{38} AND Ti^{46} FROM THE p,n REACTION ON Cl^{37} AND Sc^{45} RESPECTIVELY

by

Lieutenant Commander WILLIAM AUGUST SCHOENFELD

and

Lieutenant Commander ROBERT WAYNE DUBORG

Submitted for the degree of Master of Science in the Department of Physics on May 18, 1951

ABSTRACT

The M.I.T. Rockefeller Generator was used as a source of protons for a study of the p,n reaction on Cl^{37} and Sc^{45}. A 1.8 Kev chlorine target and a 5.0 Kev scandium target were used. The Rockefeller Generator was equipped with a proton magnetic moment resonance field control for measuring and controlling the proton energies. A long counter was used for neutron detection, the yield of which showed a number of maxima. The proton kinetic energies at which these maxima occur are tabulated, but are not corrected for the effects due to the thickness and possible surface contamination of the targets, and motion of the center of mass. These values when corrected and combined with the binding energies of a proton in the compound nuclei give the energy levels in the compound nuclei. Energy level spacings, obtained

15655

ENERGY LEVELS IN $_{29}Cu^{63}$ AND $_{31}Ga^{69}$ FROM THE p,n REACTION ON $_{29}Cu^{63}$ AND $_{30}Zn^{65}$ RESPECTIVELY

by

Lieutenant Commander CLIFTON ROBERT GOODWINDS

and

Lieutenant Commander ROBERT WATKINS BIRDSO

Submitted for the degree of Master of Science in the Department of Physics on May 15, 1951

ABSTRACT

The M.I.T. Cockcroft-Walton Generator was used as a source of protons for a study of the p,n reaction on $_{29}Cu^{63}$ and $_{30}Zn^{65}$. A 1.5 Mev carbide target and a 5.0 Mev aluminum target were used. The Cockcroft-Walton Generator was equipped with a proton magnetic moment resonance field control for measuring and controlling the proton energies. A long counter was used for neutron detection, the yield of which showed a number of maxima. The proton kinetic energies at which these maxima occur are tabulated, but are not corrected for the effects due to the thickness and possible surface contamination of the targets, and motion of the center of mass. These values when corrected and combined with the binding energies of a proton in the compound nuclei give the energy levels in the compound nuclei. Energy level spacings, obtained

from the separation of the peaks in the yield curve are also tabulated.

Chlorine was investigated from 1.550 Mev to 2.510 Mev. The observed threshold of 1.641 ± .002 Mev led to a Q value of -1.598 ± .002 Mev and a mass difference for A^{37} - Cl^{37} of .000876 ± .000005 amu. The average energy level spacing in A^{38} was 6.1 Mev.

Scandium was investigated from 2.760 Mev to 3.125 Mev. The observed threshold of 2.913 ± .003 Mev led to a Q value of -2.850 ± .003 Mev and a mass difference for Ti^{45} - Sc^{45} of .002221 ± .000006 amu. The average level spacing in Ti^{46} was 6.0 Mev.

from the magnetization of the phase in the yield stress and also variations.

Solving the linearized form 1.37) for $\Delta\tau$ at 0.01 the measured displacement of $\Delta\phi(t) \pm .001$ rad can be a value of $-1.378 \pm .006$ for and a mean difference for $\Delta T - \log T$ of $.00014 \pm .00000$ sec. The average energy level density is ΔT sec $\pm$.

Similarly we linearized from 1.40) for $\Delta\tau$ 0.01 the relative displacement of $0.013 \pm .001$ rad can be a value of $-5.180 \pm .007$ for and a mean difference for $\Delta T - \log T$ of $.00012 \pm .00000$ sec. The average level density is ΔT sec $\pm$.

TABLE OF CONTENTS

	Page
ABSTRACT	i
CHAPTER I - INTRODUCTION	1
CHAPTER II - EXPERIMENTAL ARRANGEMENT	5
General	5
Proton Energy	5
Instrumentation	6
CHAPTER III - TARGETS	12
CHAPTER IV - EXPERIMENTAL RESULTS	15
$Cl^{37}(p,n)A^{37}$	15
$Sc^{45}(p,n)Ti^{45}$	23
General	37
CHAPTER V - THEORETICAL CONSIDERATIONS	43
Neutron Energies	43
Energy Levels	45
BIBLIOGRAPHY	53
ACKNOWLEDGMENTS	55

TABLE OF CONTENTS

Page

ABSTRACT i

CHAPTER I - INTRODUCTION 1

CHAPTER II - HISTORICAL CONSIDERATIONS 3

GENERAL 3

TYPICAL SHORT SHOT 3

DEFINITIONS 6

CHAPTER III - FLUIDS 12

CHAPTER IV - EXPERIMENTAL RESULTS 15

$\mathrm{CO}_2^{(3+3)}/\mathrm{N}^{2}$ 15

$\mathrm{CO}_2^{(3+3)}/\mathrm{O}_2$ 25

GENERAL 37

CHAPTER V - THEORETICAL CONSIDERATIONS 43

DEFINITE CONDITION 43

THERMAL LATITUDE 45

THERMODYNAMICS 53

ADIABATIC EXPANSION 57

LIST OF FIGURES

		Page
Figure 1.	Neutron Yield from $Cl^{37}(p,n)A^{37}$ near Threshold	17
Figure 2.	Neutron Yield from $Cl^{37}(p,n)A^{37}$ 1.670 - 2.510 Mev	20
Figure 3.	Neutron Yield from $Cl^{37}(p,n)A^{37}$ 2.375 - 2.510 Mev	22
Figure 4.	Neutron Yield from $Sc^{45}(p,n)Ti^{45}$ 2.894 - 3.128 Mev	25
Figure 5.	Reproducibility of Peaks $Cl^{37}(p,n)A^{37}$.	39
Figure 6.	Reproducibility data $Sc^{45}(p,n)Ti^{45}$ ...	41

LIST OF FIGURES

Page

Figure 1. Electron field lines of $SU^{37}(2,1)$ under transformation 19

Figure 2. Positron field lines of $SU^{37}(2,1)$ $\lambda_4(\theta)$ = $\lambda_5(\theta)$ cos 20

Figure 3. Positron field lines of $SU^{37}(2,1)$ $\lambda_4(\theta)$ = $\lambda_5(\theta)$ sin 23

Figure 4. Electron field lines for $SU^{43}(2,1)$ $\lambda_4(\theta)$ = $\lambda_5(\theta)$ - $\lambda_7(\theta)$ cos 25

Figure 5. Non-commutativity of Yang of $SU^{37}(2,1)$. 29

Figure 6. Triplecommutativity Yang $SU^{43}(2,1)$ 33

LIST OF TABLES

Page

Table 1. Resonance Peaks in Neutron Yield from $Cl^{37}(p,n)A^{37}$ 26

Table 2. Resonance Peaks in Neutron Yield from $Sc^{45}(p,n)Ti^{45}$ 35

Table 3. Spacings in Ti^{46} 49

Table 4. Spacings in A^{38} 52

LIST OF TABLES

Page

Table 1. Frequency Data in Western Trail Area (Y_{1}, Y_{2}) 60

Table 2. Frequency Data in Western Trail Area (Y_{1}, Y_{3}) 72

Table 3. Overlaps in Y_{1} 87

Table 4. Overlaps in Y_{2} 90

CHAPTER I

INTRODUCTION

During the nineteenth century, a great deal of work was done on optical spectra and atomic energy levels. From this grew our present day quantum mechanical picture of atomic and molecular structure. The present work on nuclear energy levels is expected to lead to a similar improvement in our knowledge of nuclear structure.

One method of observing nuclear energy levels is by means of the (p,n) reaction:

$$(Z-1)^{A-1} + p \rightarrow Z^{A} \rightarrow Z^{A-1} + n + Q$$

It is experimentally known that the neutron yields from (p,n) reactions exhibit maxima at certain energies of the bombarding protons. The Breit-Wigner theory attempts to explain this as a resonance phenomenon. When the kinetic energy of the proton (Ep) approaches certain critical values, the total energy of the initial state (target nucleus plus proton) corresponds to the energy levels of the compound nucleus. However, the proton kinetic energies at which maxima in the neutron yields occur differ from these critical values because of the thickness and possible sur-

CHAPTER I

INTRODUCTION

During the nineteenth century, a great deal of work was done on optical spectra and atomic energy levels. From this grew our present day quantum mechanical picture of atomic and molecular structure. The present work on nuclear energy levels is expected to lead to a similar improvement in our knowledge of nuclear structure.

One method of observing nuclear energy levels is by means of the (p,n) reaction:

$$(Z-1)^{A-1} + p \rightarrow Z^{A} \rightarrow Z^{A-1} + n + \gamma$$

It is experimentally known that the neutron yields from (p,n) reactions exhibit maxima at certain energies of the bombarding protons. The Breit-Tuan theory attempts to explain this as a resonance phenomenon. When the kinetic energy of the proton (Zp) approaches certain critical values, the total energy of the initial state (target nucleus plus proton) corresponds to the energy levels of the compound nucleus. However, the proton kinetic energies at which maxima in the neutron yields occur differ from these critical values because of the Coulomb and possible cor-

face contamination of the target, the displacement of the peak due to the effect of neighboring peaks, and motion of the center of mass. By making corrections for these effects, and knowing the binding energy of the proton, the observed proton energies of the maxima lead to energy levels of the compound nucleus. (see diagram)

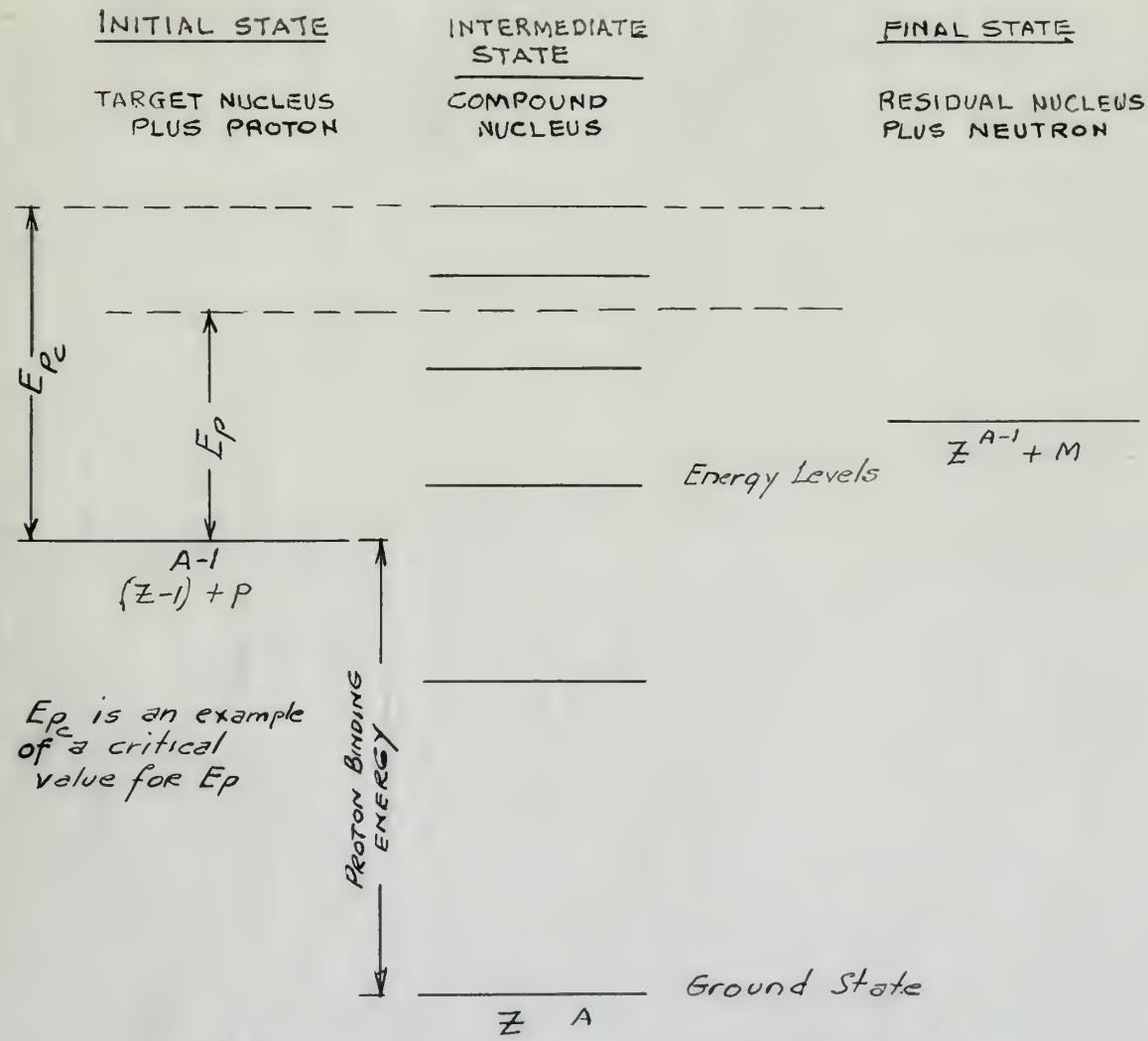

face contamination of the target, the displacement of the peak due to the effect of neighboring peaks, and masking of the border of mass. By making corrections for these effects, and knowing the binding energy of the proton, the compound proton energies of the masking lead to energy levels of the compound nucleus. (see diagram)

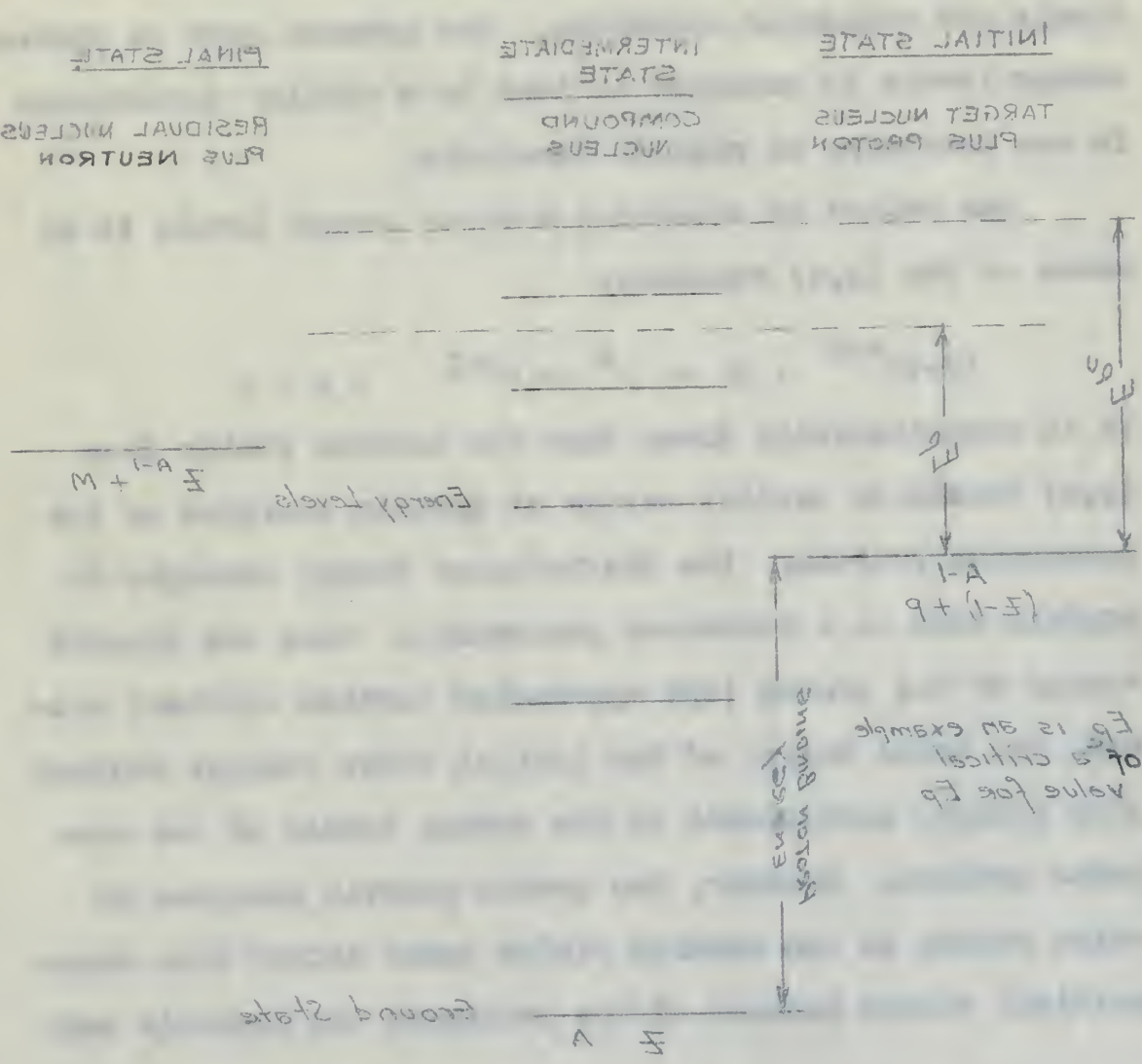

Although a number of other reactions give the same results, the (p,n) reaction was used for the following reasons. The Rockefeller generator provides a convenient source of protons of good energy resolution. The product particles, neutrons, are easily detected. Since they are uncharged, they have a long range and penetrate the target, which stops all of the bombarding protons. Thus the measured yield is all due to the neutrons as none of the protons get to the counter.

Previous work has been done on energy levels in light nuclei using the (p,n) reaction. A summary of this work is given by Richards et al (R1). The (p,n) reaction in manganese has been studied by McCue and Preston (M1), and in scandium and vanadium by Baker, Howell, Goodman and Preston (B1, B2). The latter used the M.I.T. Rockefeller generator, but a proton resonance system which controls the magnetic field has been installed subsequently. This allows much better resolution of the proton energy, which together with the use of thinner targets, results in much better resolution of the peaks in scandium.

The threshold energies of chlorine and scandium are low enough (1.6 and 2.9 Mev respectively) to permit the use of the Rockefeller generator. Although these are moderately heavy nuclei, their coulomb barriers (5.3 Mev for

Although a number of other reactions have been tested, the (p,n) reaction has been our main concern. The neutrons generated provides a convenient means of probing at high energy transitions. The neutron particles, neutrons, are easily detected. Since they are uncharged, they have a long range and penetrate the target, which stops all of the nonelastic products. Thus the observed yield is all due to the neutrons as long as the protons get to the counter.

Previous work has been done on energy levels in light nuclei using the (p,n) reaction. A summary of this work is given by Ajzenberg et al (A1). The (p,n) reaction in nuclei has been studied by Jones and Preston (J1), and in combination and comparison by Baker, Dowell, Goodman and Preston (B1, B2). The latter used the M.I.T. Moderateur generator, but a proton recoil spectrometer which controls the magnetic field has been installed subsequently. This allows much better resolution of the proton energy, which together with the use of thinner targets, results in much better resolution of the peaks in excitation.

The theoretical energies of ordinary and nonelastic are low enough (1.6 and 2.9 Mev respectively) to permit the use of the Moderateur generator. Although these are nonetheless heavy models, their nonelastic matrices (J.) may be

chlorine and 6.1 Mev for scandium) are low enough so that satisfactory yields could be obtained. The level spacings of the compound nuclei are sufficient to permit the observation of a fair number of levels under the conditions of this experiment, and targets of these elements are fairly easy to prepare from readily available materials.

chlorine and C_2 (by the reaction) are low enough so that satisfactory yields could be obtained. The level equations of the improved model are sufficient to permit the observation of a fair number of levels under the conditions of this experiment, and margins of these elements are fairly easy to compare from readily available materials.

CHAPTER II

EXPERIMENTAL ARRANGEMENT

General: The Rockefeller generator (V1, J1) is an electrostatic generator which has been adapted as a proton accelerator. The protons of desired energy were bent through 90° by a magnetic field. They then struck the target, which was composed of a layer of the desired element on a tantalum backing. The resulting neutrons were then detected by a BF_3 proportional counter, surrounded by paraffin. After amplification, the pulses were counted on a scaler.

Proton Energy: The proton energy was determined from the intensity of the magnetic field, measured by the "proton resonance method," which is described by Hadden (H3). The fundamental non-relativistic equations dealing with this measurement are given below.

The expression for the force on a charged particle moving in a magnetic field is:

$$\frac{mv^2}{r} = \frac{Bev}{c}$$

$$v = \frac{reB}{cm}$$

$$E = \frac{1}{2}mv^2 = \frac{1}{2}m\left(\frac{re}{cm}\right)^2 B^2 = k'B^2$$

$$E = k'B^2$$

m = mass of proton

v = velocity of proton

r = radius of curvature

B = magnetic field

c = velocity of light

CHAPTER II

EXPERIMENTAL ARRANGEMENT

General: The Dosmarkiles generator (Fig. 2A) is an electrostatic generator which has been adapted as a proton accelerator. The protons of desired energy were bent through 90° by a magnetic field. They then struck the target, which was composed of a layer of the desired elements on a tantalum backing. The resulting neutrons were then detected by a BF_3 proportional counter, controlled by pulsing. After amplification, the pulses were counted on a scaler.

Proton Energy: The proton energy was determined from the intensity of the magnetic field, measured by the "proton resonance method," which is described by Bethe (2)(1). The fundamental non-relativistic equations dealing with this measurement are given below.

The expression for the force on a charged particle moving in a magnetic field is:

$$\frac{mv^2}{r} = \frac{Hev}{c}$$

$$v = \frac{rHe}{mc}$$

$$H = \frac{c}{r}\sqrt{2mT} = \frac{c}{r}\sqrt{\frac{2m}{e}}\sqrt{eT} = K \cdot \sqrt{eT}$$

$$T = K \cdot H^2$$

e = mass of proton

v = velocity of proton

H = radius of curvature

r = magnetic field

c = velocity of light

The expression for the torque exerted by a magnetic field on a body of magnetic moment μ is:

$$T = B\mu \sin\theta$$

also;

$$T = \frac{dp}{dt} = \frac{\mu}{\gamma} \sin\theta\,(2\pi f)$$

$$\gamma B = 2\pi f$$

$$E = kf^2$$

e = charge on electron

E = energy of proton

T = torque

μ = magnetic moment of proton

θ = angle between μ (or I) and B

p = angular momentum of proton

f = frequency of precession of proton in magnetic field

γ = gyromagnetic ratio of a proton $= \frac{\mu}{I}$

I = proton angular momentum

k = constant

k' = constant

Therefore, the energy of the protons is proportional to the square of the frequency, which is measured with a frequency meter. For the determination of the proportionality constant, k, which relates proton energy to frequency, the Li^7 threshold (E_o = 1.8822 Mev as measured by Herb (H1, H2)) was used. The frequency corresponding to this E_o is f_o = 10.485 mc. Therefore,

$$E_o = kf_o^2$$

$$k = E_o/f_o^2 = \frac{1.8822}{(10.485)^2} = 0.017121 \text{ Mev/(mc)}^2$$

$$= 17.121 \text{ kev/(mc)}^2$$

The expression for the torque exerted by a magnetic field on a body of magnetic moment μ is:

$$T = B\mu \sin\theta$$

also:

$$T = \frac{dp}{dt} = \frac{h}{2\pi} \sin\theta \, (2\pi\nu)$$

$$p = 2\pi\nu$$

$$E = h\nu$$

θ = angle between μ (or I) and B

p = angular momentum of proton

ν = frequency of precession of proton in magnetic field

γ = gyromagnetic ratio of a proton $= \frac{\mu}{I}$

I = proton angular momentum

K = constant

K' = constant

e = charge on electron

M = mass of proton

T = torque

μ = magnetic moment of proton

Therefore, the energy of the protons is proportional to the square of the frequency, which is measured with a frequency meter. For the determination of the proportionality constant, K, which relates proton energy to frequency, the H_2^+ threshold (E_0 = 1.6022 kev as measured by Nier (N3, N2)) was used. The frequency corresponding to this E_0 is ν_0 = 10.1.55 mc. Therefore,

$$E_0 = K\nu_0^2$$

$$K = E_0/\nu_0^2 = \frac{1.6022}{(10.1.55)^2} = 0.01721 \text{ kev}/(\text{mc})^2$$

$$= 17.121 \text{ kev}/(\text{mc})^2$$

This value of k was used in the present work. Substantial changes in k result from readjustments of the proton resonance apparatus. In addition, there are minor variations in k as discussed below.

The accuracy of the measured value of the energy of the beam is limited because of the following:

1. A possible variation of the value of k with energy. This has been studied by Preston and Stelson (P1) using the mass 1 and 2 beams on a (p,γ) resonance in aluminum at 993 Kev. The error was found to be less than 1 part in 5,000 in the absolute value of the beam energy.

2. The frequency can be measured to 1 part in 100,000, and since the energy is proportional to the square of the frequency, this causes an error of 2 parts in 100,000 in the value of the beam energy.

3. The width of the beam-defining slits could permit a maximum error of 15 parts in 10,000 in the beam energy, for 40 mil slits, and 7.5 parts in 10,000 for 20 mil slits. The actual error is probably less than half of these. This was determined by Preston and Stelson (P1).

4. The value of k is determined from the (p,n) threshold of Li^7 (H1, H2), and this causes an error of 1 part in 1000 in the beam energy because of the uncertainty in the Li^7 threshold.

This value of k was used in the previous work. Potentiometer charges in k result from modifications of the circuit resonance characteristics. In addition, there are minor variations in k as discussed later.

The accuracy of the measured value of the energy of the beam is limited because of the following:

1. A possible variation of the value of k with energy. This has been studied by Treasure and Jenkins [12] using the mode 1 and 2 beams on a [0,4] resonance in aluminum at 297 kev. The error was found to be less than 1 part in 2,000 in the absolute value of the beam energy.

2. The frequency can be measured to 1 part in 100,000, and since the energy is proportional to the square of the frequency, this causes an error of 2 parts in 100,000 in the value of the beam energy.

3. The width of the beam-deflection plate should provide a maximum error of 15 parts in 10,000 in the beam diameter, for 40 mil slits, and 4.5 parts in 10,000 for 20 mil slits. The actual error is probably less than half of these. This was determined by Preston and Jenkins [13].

4. The value of k is determined from the [0,4] resonance of Li^7 (E1, M2), and this causes an error of 1 part in 1000 in the beam energy because of the uncertainty in the Li^7 theory.

5. A drift in the value of k since the last calibration, using the Li^7 threshold, may cause an error of 1 part in 2000 in the beam energy. The reason for this drift is unknown.

6. The use of the non-relativistic equation introduces an error. The calibration is such that this error is zero at E_0. According to Preston (P2) the error is about 1.7 Kev at a proton energy of 3.1 Mev (the highest energy used), and is less for lower energies.

In addition to the above, which cause an uncertainty in the beam energy prior to striking the target, the thickness and surface contamination of the target cause a further uncertainty in the energy of the reacting protons. Because of the care used in the preparation and use of the targets, and the ability to reproduce data, it was assumed that surface contamination was negligible, and did not build up during the experiment. The upper limit to the target thickness, discussed in a later section, sets an upper limit to the uncertainty in the energy of the protons due to this cause. Considering all of these factors, it is estimated that the values of the proton energies, relative to Herb's measured value of the Li^7 (p,n) threshold, are accurate to within 0.1%.

<u>Instrumentation</u>: The long counter used to detect

5. A drift in the value of E alone has last indefinitely, using the H_1^T theoretical, but causes an error of 1 part in 3000 in the beam energy. The present the field drift is unknown.

6. The use of the monochromatic scattering technique causes no error. The multiplicity is such that this error is zero at E_0, decreasing to fractions (1%) this order in about 1.5 Mev at a proton energy of E_0 (for this model measurement model), and is then low lower energies.

In addition to the above, noting cause an uncertainty in the beam energy prior to predicting the targets, the triangle and uniform accelerations of the target cause a certain uncertainty in the energy of the scattering protons. Because of the zero dead in the proportion and the of the targets, and the utility to repeatedly done, it was assumed that perhaps correlation was negligible, and the sum taking up during the experiment. The upper limit to the target thickness, discussed in a later section, were so upper limit in the uncertainty in the energy of the protons due to this cause. Considering all of these factors, it is estimated that the values of the proton energies relative to those measured value of the H_1^T (p,n) threshold, are accurate to within 0.1%.

Instrumentation: The long counter used in taking

neutrons consisted of an enriched BF_3 counter tube, surrounded by paraffin, similar to that described by Hansen and McKibben (H4). The paraffin cylinder was 8" in diameter and 10" in length, and was surrounded by cadmium. This counter differed from that of Hansen and McKibben in that no holes were provided in the face of the paraffin. The counter tube had the following specifications:

Outside diameter	1"
Wall Thickness	0.042" of brass
Active volume	10" in length
Center Wire	2 mil tungsten
Filling	55 cm of Hg of 96% enriched $B^{10}F_3$
Operating voltage	2200 volts

The long counter was mounted with the axis of the cylinder perpendicular to the direction of the proton beam as shown in the sketch below. It was used in this position in order to subtend as large a solid angle as possible. Since the neutrons may be emitted anisentropically in the center of mass system, this arrangement reduced the possibility of not detecting peaks in the yield curves because of the angular distribution of the emitted neutrons. It was checked at the start and finish of each individual run with a standard Ra-Be neutron source.

neutrons emanating at an angle of 90° another time, were treated in parallel similar to the deflection of neutrons and electrons (24). The parallel cylinder was 8" in diameter and 30" in length, and was surrounded by neutrons. This counter differed from that of Chadwick and Goldhaber in that the holes were parallel in the face of the cylinder. The counter tube had the following specifications:

Outside diameter	1"
Wall thickness	0.020" of brass
Active volume	30" in length
Center wire	6 mil tungsten
Filling	22 mm Hg of 90% enriched He^3
Operating voltage	2800 volts

The long counter was counted with two rows of ten counters perpendicular to the direction of the proton beam as shown in the sketch below. It was used in this position in order to measure as large a solid angle as possible. Since the neutrons may be emitted anisotropically in the center of mass system, this arrangement counted the possibility of not detecting peaks in the field energy because of the angular distribution of the emitted neutrons. It was shielded on the sides and floor of such individual row with a removed Be-Be neutron source.

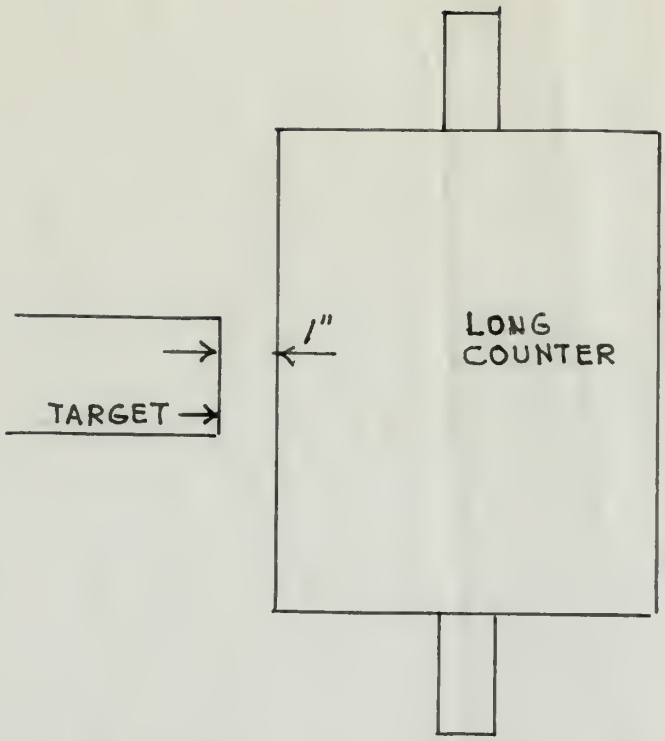

The data on the other instruments used are:

Preamplifier: Laboratory for Nuclear Science and Engineering, M.I.T., Model 100.

Amplifier: Laboratory for Nuclear Science and Engineering, M.I.T., Model 100. The preamplifier and amplifier are discussed fully in Elmore and Sands (E1). The amplifier had a gain of 10,000, a rise time of 0.5 micro seconds, and a clipping time of 2 micro seconds.

Scaler: Atomic Instrument Co. Model 105. Resolving time -- 5 micro seconds.

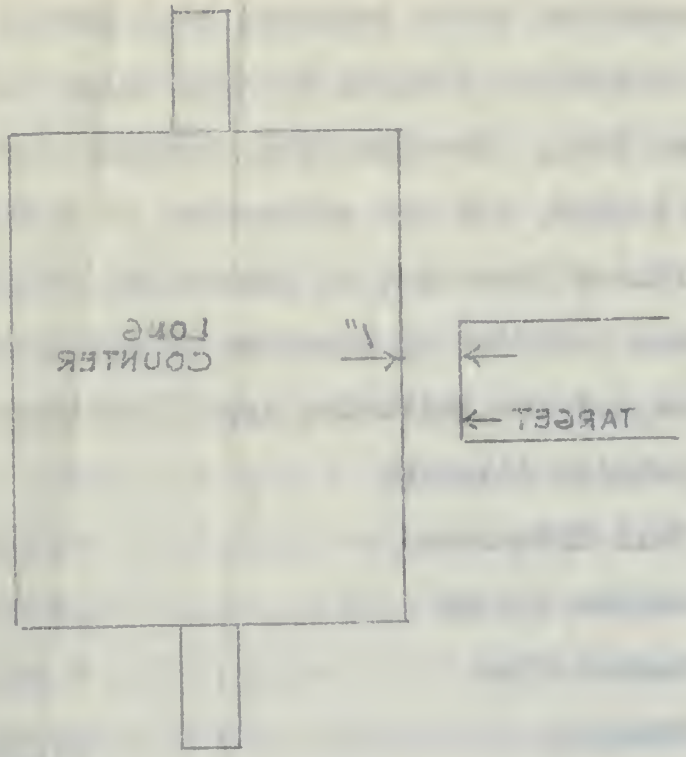

The data on the other instruments used are:

Preamplifier: Laboratory for Nuclear Science and Engineering, N.I.T., model 100.

Amplifier: Laboratory for Nuclear Science and Engineering, N.I.T., model 100. The preamplifier and amplifier are discussed fully in Zinore and Banks (21). The amplifier had a gain of 10,000, a rise time of 0.5 micro seconds, and a clipping time of 2 micro seconds.

Scaler: Atomic Instrument Co. model 105. Resolving time -- 2 micro seconds.

Regulated High Voltage Supply: M.I.T. Servo Lab., Electronic Nuclear Instrument Project. Electronically stabilized.

Frequency Meter: General Radio Co. Model 271. 160 kc -- 15 mc.

The amplifier, preamplifier, and high voltage supply were run from a voltage regulating transformer with a sine wave output.

Regulated High Voltage Supply: M.I.T. Servo Lab., Electronic Nuclear Instrument Project, Instrumentality established.

Frequency meter: General Radio Co. Model 477, 160 kc - 15 mc.

The amplifier, preamplifier, and high voltage supply were run from a voltage regulating transformer with a sine wave output.

CHAPTER III

TARGETS

The scandium targets were made from Sc_2O_3 prepared by Johnson and Malthey and Co., Ltd. of London. It was obtained from the Jarrell Ash Co. of Boston, Massachusetts. The oxide was certified "spectrographically standardized." Baird Associates of Cambridge, Massachusetts made the targets using the method developed by Baker and Howell (B2). The scandium targets were not thicker than 5 Kev. This upper limit was determined from the width of the narrowest peak measured at half its maximum amplitude. A target used by Baker et al was available, but almost no yield of neutrons was obtained from this target. Apparently the targets deteriorate over a period of time, so that targets used in this work were made very shortly before being used. Between runs they were stored in a vacuum to minimize any contamination or oxidation. While being bombarded with protons, the targets were continuously cooled by a stream of air to reduce evaporation of the scandium. In order to ensure that no changes took place in the target during a run, a measurement of the same peak was made at the start and finish of each individual run. Using these methods, no difficulties were encountered with the targets.

SECTION III

Results

The meadlum burgets were made from "Sun", procured by Sponsors and Fishing and Co., Ltd. of London. It was obtained from the Aircraft Ad Co. of Sheffield, Lancashire. The cells are specified "quadruple-polarity standard". Being impregnated of Gonderfiqu, Bassalmanzie made the burgets with using the method developed by Baker and Sewell (20). The meadlum burgets were not thicker than 5 mm. This upper limit was determined from the width of the surrounded peak measured at half the maximum amplitude. A burgets used by Baker at al was available, but always no yield of measures was obtained from this burgets. Apparently the burgets deteriorate over a period of time, so that burgets used in this work were made very shortly before being used. Between runs they were stored in a vacuum to minimize any contamination or oxidation. While being produced with pressure, the burgets were mechanically sealed by a stream of air to reduce evaporation of the meadlium. In order to ensure that no samples took place in the burgets during a run, a measurement of the mass peak was made at the start and finish of each individual run. Using these methods, no difficulties were encountered with the burgets.

The chlorine targets were made from NaCl, prepared by Johnson and Matthey and Co. Ltd. of London. It was obtained from the Jarrell Ash Co. of Boston, Massachusetts. The NaCl was of a high degree of purity, and was certified "spectrographically standardized." Lines of silver, copper, and magnesium were faintly visible. Lines of calcium were very faintly visible. Iron and silicon lines were detected, but were fainter than those seen using plain electrodes, so their presence is doubtful. The above is from the report on the NaCl issued by the Johnson and Matthey Co.

Baird Associates of Cambridge, Massachusetts made the chlorine targets, using the method described by Baker and Howell (B2) for the preparation of vanadium targets. The threshold energies of Na (W2) and Cl^{35} (W3) were well above the energies used, so that they did not enter into the reaction. The target used for the energy level measurements in the chlorine work was not thicker than 1.6 Kev. The target used near threshold was not thicker than 4.3 Kev. At first, difficulty was experienced with the chlorine targets changing during a run. When checking a peak at the end of a run, its maximum amplitude would be much less than it had been at the start of the run. However, by keeping the beam current below 3 micro amperes, and using a spray of cooling water on the target, in addition to taking the precautions

The solution lacking was some first hand, informed by theories and relating the ideas of Lorenz. It was obtained upon his -Central use the of Spring, Representative. The idea was of a kind phase of "rolling", and his analogies "psychologically transformations." Image of civil, economic and sociological were relatively vivid. Image of political were very quite vivid. Then the citizen image was lacking, but were talking about lower power units, state, tribes, or, in short groups in America. The study is from the report on the data learned by the Lorenz and Lorenz Jr.

Social conditions of Americans Representative said the political system, which has taking existing to Tonge and Dowell (10) for the properties of Political Theory. The sociological analysis of Mr (10) and Mr.[12] (10) were well above the analysis made, by Tonge and Dowell and not quite like the analysis. The survey made for the study Lorenz representative in the allocation which was not different than Mr Tonge. The text and sociological was the relative than Mr Dowell. It clearly difference was interpreted with the relative Theory although lacking a year. Lorenz showing a good of the and of a map, the political conditions would be good lack then it was lost at the which of the map. However, by imagine the same political belief) which economy, and using a study of political when on the lorenz. In addition to telling the Representative

described for the scandium targets, this difficulty was overcome.

It was assumed that effects due to surface contaminations on the chlorine and scandium targets were negligible. This assumption is based on the method used to make the targets, the fact that they were stored in vacuum in between runs, and the ability to reproduce data.

described for the anesthesia surgery, this difficulty was overcome.

It was assumed that efforts due to surface anesthesia on the cutaneous and association surgeries were negligible. This assumption is based on the medical need to relax the surgery, the fact that they were placed in vicinity in between zones, and the utility of injection data.

CHAPTER IV

EXPERIMENTAL RESULTS

$Cl^{37}(p,n)A^{37}$: The neutron yield from the chlorine target was measured over an energy range from 1.550 Mev to 2.510 Mev.

From 1.550 Mev to 1.641 Mev, the neutron yield observed was constant at a background of 0.1. As the proton energy was increased, the neutron yield started to increase. This increase occurred just above the threshold of the reaction. Figure 1 shows a plot of the results near the threshold, from 1.630 Mev to 1.700 Mev. The region from 1.550 Mev to 1.630 Mev is not shown in this figure, since the yield was a constant as previously mentioned. The threshold[1] for the reaction was taken as the energy at which the rise in the yield curve started, or a value of 1.641 ± 0.002 Mev. This error is due to the 0.1% uncertainty in the proton energy, as previously discussed. This value agrees very closely with 1.640 ± 0.004 Mev as measured by Richards et al (R1).

---

1. For neutrons emitted at 0° with respect to the direction of incident protons.

CHAPTER IV

CONCLUSIONS AND RESULTS

Gd^{99}(p,n)Dy^{99}: The neutron yield from the bombing target was measured over an energy range from 1.152 Mev to 2.510 Mev.

From 1.320 Mev to 1.641 Mev, the neutron yield observed was constant at a background of 0.1. As the proton energy was increased, the neutron yield started to increase. This increase reached four times the background of the reaction. Figure 1 shows a plot of the variation past the threshold, from 1.630 Mev to 1.700 Mev. The region from 1.320 Mev to 1.630 Mev is not shown in this figure, since the yield was a constant as previously mentioned. The threshold[1] for the reaction was taken as the energy at which the rise in the yield curve occurred, at a value of 1.641 ± 0.001 Mev. This error is due to the 0.1% uncertainty in the beam energy, as previously discussed. This value agrees very closely with 1.640 ± 0.004 Mev as measured by Blackwell et al [11].

---

1. The neutron energy quoted is 0° with respect to the direction of incident protons.

Figure 1

NEUTRON YIELD FROM $Cl^{37}(p,n)A^{37}$
NEAR THRESHOLD

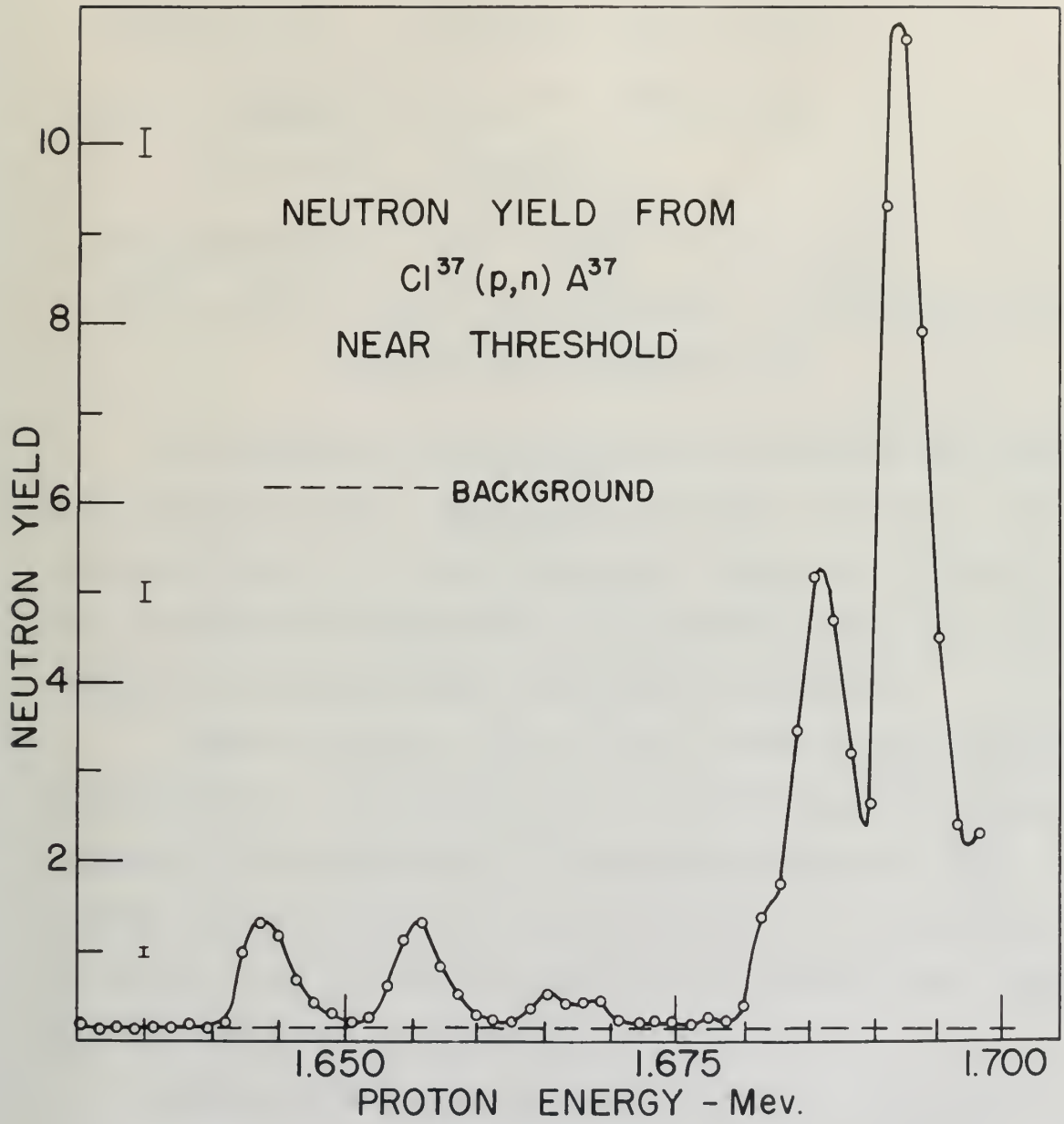
NEUTRON YIELD FROM
Cl37 (p,n) A37
NEAR THRESHOLD
BACKGROUND
NEUTRON YIELD
10
8
6
4
2
1.650
1.675
1.700
PROTON ENERGY - Mev.

$Cl^{37}(p,n)A^{37}$ threshold = 1641 ± 2 Kev

$$- Q = \frac{36.9775}{37.9856}(1641 \pm 2) = 1598 \pm 2 \text{ Kev}$$

$$= 0.001716 \pm 0.000002 \text{ amu}$$

Mass difference[2] $(A^{37} - Cl^{37}) = - Q - (n-p)$

$$(A^{37} - Cl^{37}) = 0.001716 \pm 0.000002 - (0.000840 \pm 0.000005) \quad (B3)$$

$$= 0.000876 \pm 0.000005 \text{ amu}$$

The background was determined by measuring the counting rate obtained when a pure tantalum target was used. It is shown on Figure 1. The experimental points are shown by the circles. The magnitude of the probable error in these points is indicated along the axis of ordinates.

Figure 2 shows a plot of the results from 1.670 Mev to 2.510 Mev. The background was omitted from this curve because it was negligible. The probable error at high yields is indicated, but at low yields it is too small to be shown. For the sake of clarity, the experimental points are not indicated on Figure 2.

Figure 3, the region from 2.375 Mev to 2.510 Mev, plotted to a larger scale, shows experimental points. The probable error of these points is less than the size of the circles indicating the points. This plot is included to

---

2. The effect of the electron binding energies was neglected as they were of the order of electron volts, whereas the uncertainty in the value of Q is of the order of Kev.

$$\sigma_{37}(p,\alpha)_{37} \qquad \text{microbarns} = 1861 \pm 2 \text{ kev}$$

$$= 0 = \frac{26.2775}{37.1230}\,(1861 \pm 2) = 1394 \pm 2 \text{ kev}$$

$$= 0.001710 \pm 0.000002 \text{ amu}$$

$$\text{Mass difference}^{3} \quad [A_{37} - \sigma_{37}] = - 0 - (p-n)$$

$$(A_{37} - \sigma_{37}) = 0.001710 \pm 0.000002 - (0.000840 \pm 0.000002)^{(20)}$$

$$= 0.000870 \pm 0.000002 \text{ amu}$$

The background was determined by measuring the counting rate obtained when a pure boronium target was used. It is shown on Figure 1. The supertheoretical points are shown by the circles. The magnitude of the probable error in these points is indicated along the axis of ordinates.

Figure 2 shows a plot of the ranges from 1.970 mev to 2.310 mev. The background was omitted from this curve because it was negligible. The probable error of high yields is indicated, but at low yields it is too small to be shown. For the sake of clarity, the supertheoretical points are not indicated on Figure 2.

Figure 3, the region from 2.295 mev to 2.310 mev, plotted to a larger scale, shows supertheoretical points. The probable error of these points is less than the size of the circles indicating the points. This plot is included to

---

3. The effect of the electron binding energies was neglected as they were of the order of electron volts, whereas the uncertainty in the value of Q is of the order of kev.

Figure 2

NEUTRON YIELD FROM $Cl^{37}(p,n)A^{37}$

1.670 - 2.510 Mev.

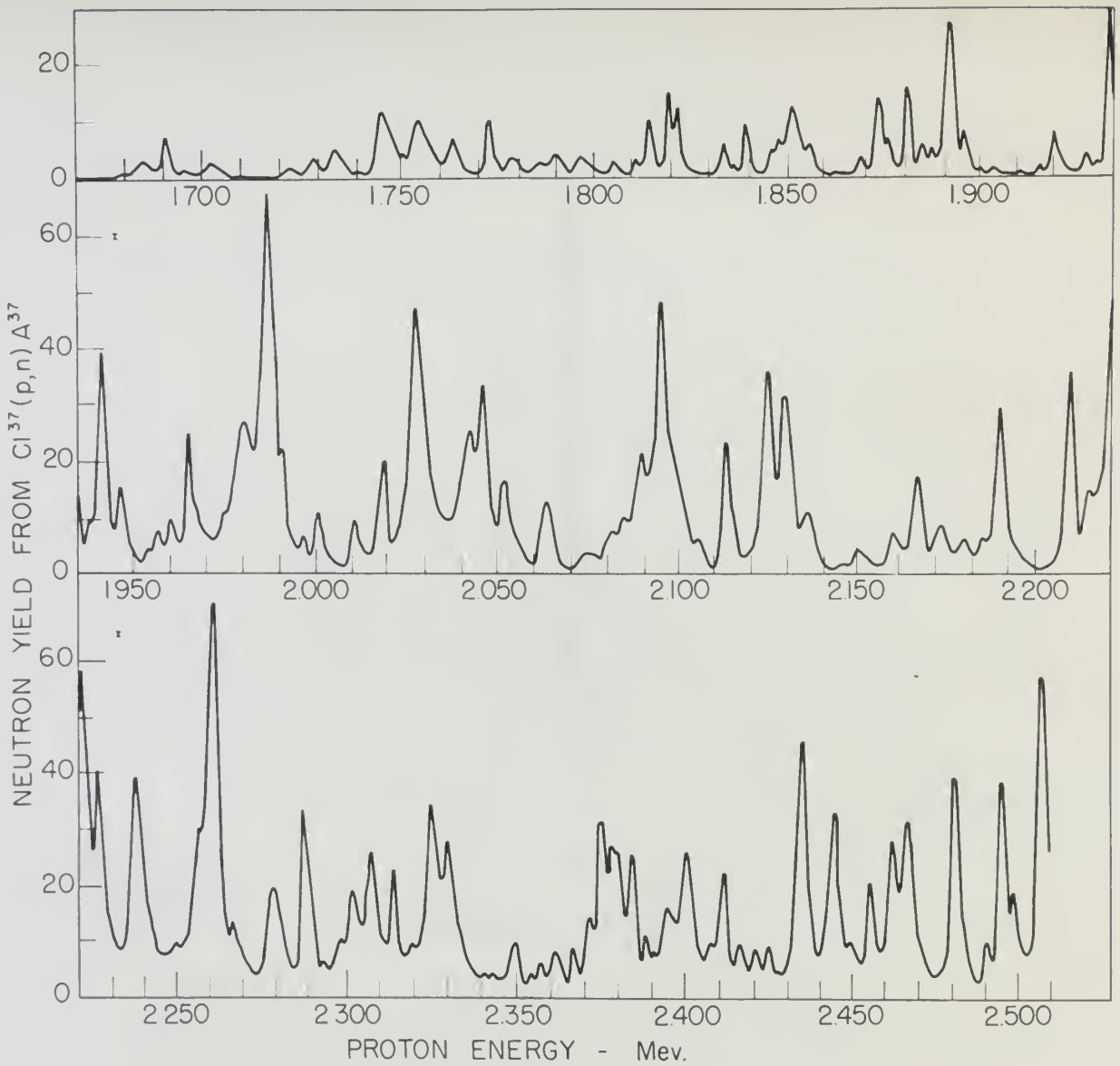
NEUTRON YIELD FROM $Cl^{37}(p,n)A^{37}$
PROTON ENERGY - Mev.
0
20
40
60
1.700
1.750
1.800
1.850
1.900
1.950
2.000
2.050
2.100
2.150
2.200
2.250
2.300
2.350
2.400
2.450
2.500

Figure 3

NEUTRON YIELD FROM $Cl^{37}(p,n)A^{37}$

2.375 - 2.510 Mev.

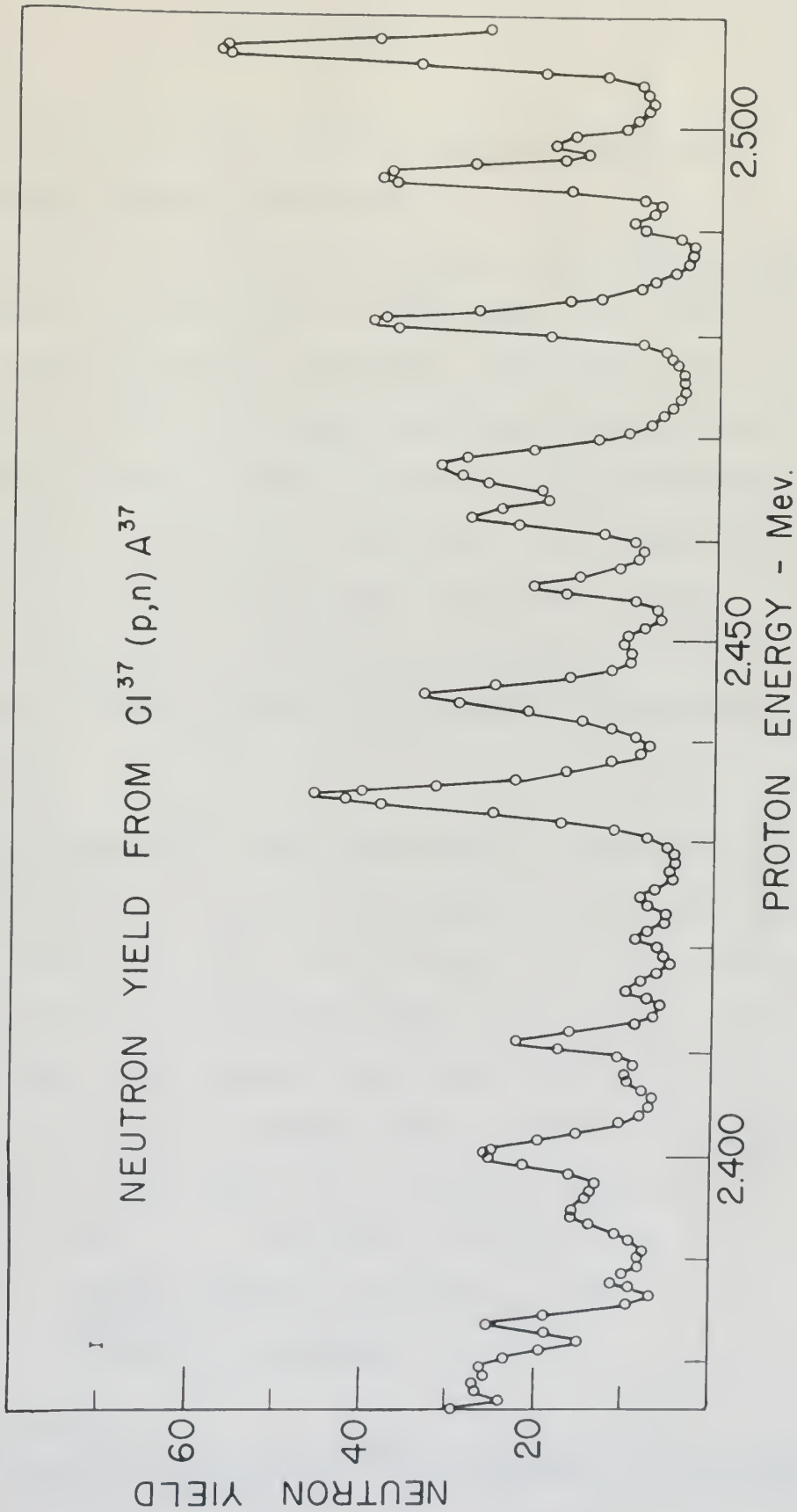
NEUTRON YIELD FROM Cl^{37} (p,n) A^{37}
NEUTRON YIELD
60
40
20
2.400
2.450
2.500
PROTON ENERGY - Mev.

show the spacing of the points, and is typical of the entire energy region investigated.

Table 1 lists all of the peaks in the neutron yield. The narrowest peak found, at 1.839 Mev, had a width of 1.8 Kev at half its maximum amplitude. This width was due to the energy spread, the target thickness, and the actual width of the level. Thus this value of 1.8 Kev sets an upper limit to the target thickness. The target thickness, measured in Kev, decreases with increasing energy. If the energy spread remains constant, the greater width of other peaks would be due to an actual increase in the width of the levels.

<u>$Sc^{45}(p,n)Ti^{45}$</u>: From 2.760 Mev to 2.913 Mev, the yield from the scandium target was practically constant, varying from 2.3 to 3.0 $\pm$ 0.07. At 2.913 Mev the yield rose sharply, indicating that the threshold[3] for the reaction is at 2.913 $\pm$ 0.003 Mev. This agrees fairly well with the value of 2.85 Mev obtained by Taschek (T1). A plot of the results from 2.894 Mev to 3.128 Mev is shown in Figure 4.

$Sc^{45}(p,n)Ti^{45}$ threshold = 2913 $\pm$ 3 Kev

$$- Q = \frac{44.966}{45.974}(2913 \pm 3) = 2850 \pm 3 \text{ Kev}$$

$$= 0.003061 \pm 0.000003 \text{ amu}$$

---

3. For neutrons emitted at 0° with respect to direction of incident protons.

show the spacing of the peaks, and is typical of the excite energy region investigated.

Table 1 lists all of the peaks in the neutron yield. The narrowest peak found, at 1.670 Mev, had a width of 1.8 Mev at half its maximum amplitude. This width was due to the energy spread, the target thickness, and the natural width of the level. Thus this value of 1.8 Mev acts as upper limit to the target thickness. The target thickness, measured in Mev, decreases with increasing energy. If the energy spread remains constant, the greater width of other peaks would be due to an actual increase in the width of the levels.

$\underline{Go^{65}(p,n)Ti^{65}}$: From 2.700 Mev to 2.913 Mev, the yield from the monitor target was practically constant, varying from 2.3 to 3.0 ± 0.07. At 2.913 Mev the yield rose sharply, indicating that the threshold[3] for the reaction is at 2.913 ± 0.003 Mev. This agrees fairly well with the value of 2.85 Mev obtained by Tanabe (71). A plot of the results from 2.894 Mev to 3.112 Mev is shown in Figure 4.

$Go^{65}(p,n)Ti^{65}$ threshold - 2913 ± 3 Mev

$= Q - \frac{1.4 \times 934}{65 \times 934}(2913 \pm 3) = 2850 \pm 3$ Kev

$= 0.00706 \pm 0.00007$ amu

---

3. For neutrons emitted at 0° with respect to direction of incident protons.

Figure 4

NEUTRON YIELD FROM $Sc^{45}(p,n)Ti^{45}$

2.894 - 3.128 Mev.

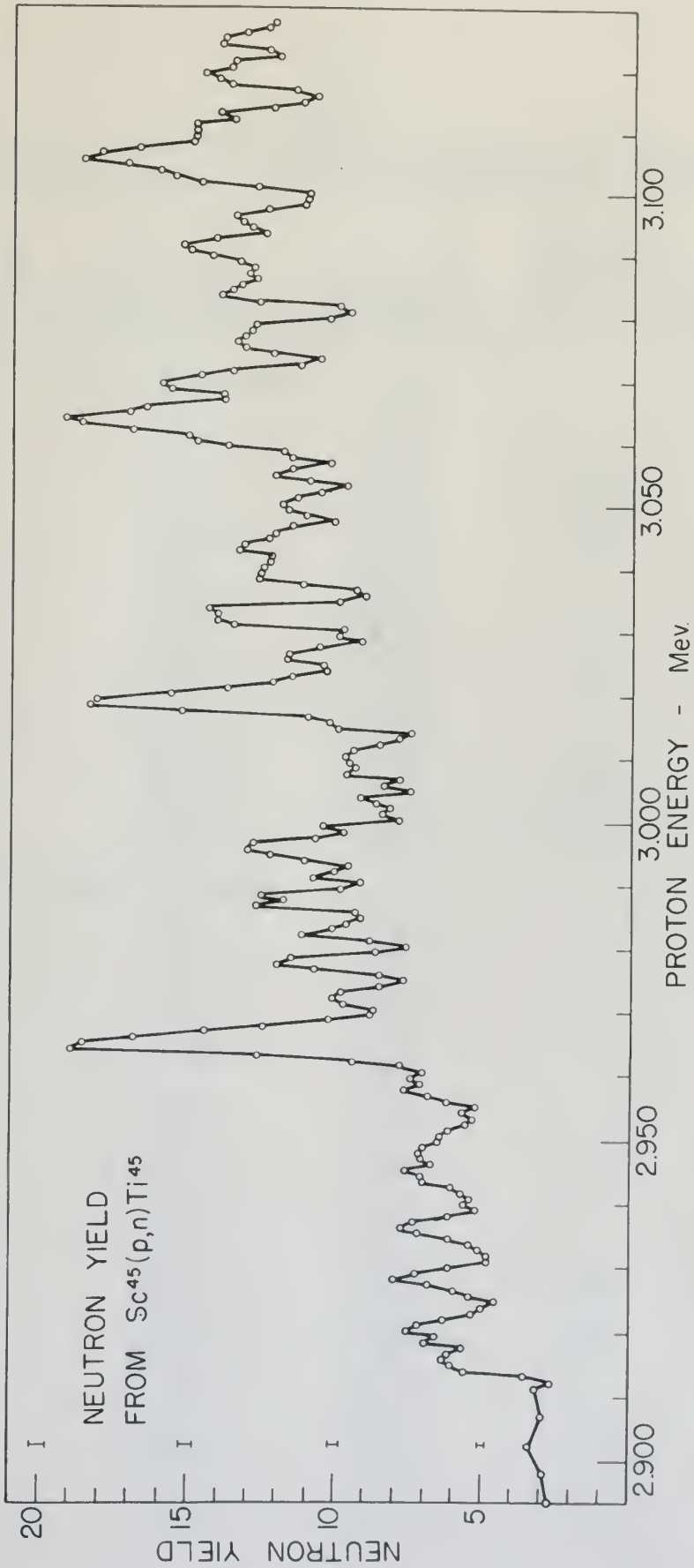
NEUTRON YIELD
FROM $Sc^{45}(p,n)Ti^{45}$
NEUTRON YIELD
20
15
10
5
2.900
2.950
3.000
3.050
3.100
PROTON ENERGY - Mev.

TABLE 1
RESONANCE PEAKS IN NEUTRON YIELD FROM $Cl^{37}(p,n)A^{37}$
Error in E ± 0.1%, relative to $Li^{7}(p,n)$ threshold

Frequency of peak - mc.	Energy of peak - Mev.	Amplitude of peak	Width at half max. - Kev.	Separation from next peak - Kev.
Thick target - near threshold:				
9.800	1.644	1.3	4.3	11
9.831	1.655	1.3	4.3	11
9.860	1.666	0.5		3
9.871	1.669	0.4		9
9.897	1.678	0.25		4
9.910	1.682	1.5		4
9.922	1.686	5.3	5.0	6
9.939	1.692	11.3	4.4	
Thin target - entire range:				
9.799	1.644	1.0		11
9.834	1.655	1.0		11
9.864	1.666	0.5		3
9.873	1.669	0.5		9
9.900	1.678	0.2		4
9.912	1.682	1.2		4
9.924	1.686	3.5	4.9	5
9.940	1.691	7.5	1.8	5
9.954	1.696	2.0		7
9.973	1.703	3.2	4.1	19
10.030	1.722	2.0	4.7	7

TABLE 1

RESONANCE PEAKS IN ELASTIC YIELD FROM $O_2^{32}(p,n)S^{32}$
Error is $\pm\frac{1}{2}$ 0.15, relative to $Li^7(p,n)$ threshold

Frequency of peak - mc.	Energy of peak - Mev.	Amplitude of peak	Width at half max. - Kev.	Importation from next peak - Mev.
Thick target - near threshold:				
9.200	1.644	1.1	6.1	11
9.231	1.655	1.1	6.1	11
9.260	1.666	0.5		7
9.273	1.669	0.4		7
9.297	1.678	0.25		4
9.310	1.682	1.5		6
9.322	1.686	5.1	5.0	6
9.339	1.692	11.1	6.4	
Thick target - entire range:				
9.279	1.644	1.0		11
9.296	1.655	1.0		11
9.266	1.666	0.5		7
9.273	1.669	0.5		7
9.300	1.678	0.2		4
9.312	1.682	1.2		4
9.324	1.686	3.5	4.5	5
9.340	1.692	7.5	1.4	5
9.354	1.696	2.0		7
9.373	1.703	3.2	4.1	19
10.030	1.734	2.0	4.7	7

TABLE 1 (continued)

Frequency of peak - mc.	Energy of peak - Mev.	Amplitude of peak	Width at half max. - Kev.	Separation from next peak - Kev.
10.050	1.729	3.5	3.6	5
10.064	1.734	5.5	4.0	7
10.084	1.741	1.5		5
10.099	1.746	12.5	4.3	5
10.115	1.751	5.0		4
10.126	1.755	10.5	5.1	9
10.151	1.764	7.0	3.2	9
10.177	1.773	10.5	2.3	5
10.192	1.778	4.2	4.1	8
10.213	1.786	3.2		3
10.224	1.789	4.6		7
10.243	1.796	4.4	4.3	9
10.267	1.805	3.5	2.3	5
10.283	1.810	4.3		4
10.293	1.814	11.0	2.7	5
10.307	1.819	15.5		2
10.313	1.821	12.5		12
10.348	1.833	7.0		3
10.355	1.836	2.5		3
10.363	1.839	10.0	1.8	7
10.383	1.846	5.5		2

TABLE I (continued)

Frequency of peak - mc/s.	Energy of peak - Mev/s.	Amplitude of peak	Width at half max. - Kev/s.	Equivalent dose rate peak - rem/s.
10.050	1.727	3.5	3.6	4
10.064	1.734	5.5	4.0	7
10.066	1.741	1.5		2
10.099	1.746	12.5	6.3	5
10.113	1.753	3.0		4
10.130	1.755	10.5	5.1	7
10.151	1.764	7.0	3.8	3
10.177	1.773	10.5	2.3	5
10.192	1.776	4.5	4.2	2
10.213	1.786	3.5		3
10.234	1.797	4.6		7
10.243	1.796	4.4	4.3	3
10.257	1.805	3.5	2.3	3
10.283	1.820	4.3		4
10.313	1.834	13.0	2.7	3
10.327	1.839	15.5		2
10.413	1.873	14.5		13
10.246	1.833	7.5		1
10.355	1.876	4.3		3
10.363	1.879	10.0	1.8	7
10.369	1.882	5.5		2

TABLE 1 (continued)

Frequency of peak - mc.	Energy of peak - Mev.	Amplitude of peak	Width at half max. - Kev.	Separation from next peak - Kev.
10.389	1.848	7.2		3
10.398	1.851	13.0	4.1	4
10.410	1.855	6.5		7
10.430	1.862	1.5		7
10.448	1.869	4.3	3.1	4
10.460	1.873	14.0	2.2	3
10.467	1.876	7.5		5
10.481	1.881	17.0	2.2	4
10.493	1.885	6.5		2
10.499	1.887	6.2		5
10.512	1.892	27.5	3.2	4
10.523	1.896	8.5		4
10.535	1.900	2.0		3
10.544	1.903	2.5		7
10.564	1.910	2.5		6
10.578	1.916	3.0		3
10.588	1.919	9.0	2.9	9
10.612	1.928	4.7		3
10.621	1.931	3.5		3
10.628	1.934	30.5	2.0	4
10.640	1.938	9.5		4

TABLE I (continued)

Frequency of mark - ν_0	Energy of mark - E_0	Width of mark at half max.	Width as half max. - ΔE_0	Separation from next mark - $\Delta\nu_0$
10.320	1.242	7.2		3
10.320	1.271	13.3	4.4	4
10.430	1.033	6.5		4
10.430	1.062	1.5		7
10.444	1.065	4.3	3.4	4
10.460	1.073	14.0	2.2	3
10.467	1.076	7.5		3
10.471	1.081	17.0	2.2	4
10.472	1.085	6.5		3
10.479	1.087	6.2		3
10.512	1.092	29.5	3.2	4
10.513	1.095	6.5		4
10.515	1.099	2.0		3
10.544	1.101	5.5		4
10.564	1.110	2.5		4
10.574	1.116	3.0		3
10.584	1.119	7.0	2.4	4
10.612	1.126	4.7		2
10.621	1.131	3.3		3
10.624	1.134	30.3	2.4	4
10.640	1.138	9.3		4

TABLE 1 (continued)

Frequency of peak - mc.	Energy of peak - Mev.	Amplitude of peak	Width at half max. - Kev.	Separation from next peak - Kev.
10.649	1.942	40.0	2.3	5
10.664	1.947	15.5		8
10.685	1.955	4.5		2
10.691	1.957	8.2		4
10.701	1.961	10.2		4
10.714	1.965	25.0	2.9	11
10.742	1.976	11.8		5
10.756	1.981	27.5		6
10.772	1.987	67.5	4.2	4
10.784	1.991	23.0		6
10.800	1.997	7.0		4
10.810	2.001	11.5	3.3	10
10.838	2.011	9.5	3.4	8
10.858	2.019	20.5	3.2	8
10.881	2.027	47.5	4.5	16
10.923	2.043	26.0		3
10.932	2.046	34.5		6
10.948	2.052	17.5	4.3	12
10.980	2.064	13.0	3.9	13
11.013	2.077	3.5		5

Table 1 (continued)

Frequency of Peak - Sec.	Energy of Peak - Ft.-Lb.	Amplitude of Peak	Ties at Half Max. - Ft.	Separation from Peak - Ft.
10.649	1.942	40.0	2.3	3
10.664	1.947	15.5		6
10.685	1.953	4.5		3
10.691	1.957	8.2		4
10.701	1.963	10.2		4
10.714	1.965	33.0	2.9	11
10.742	1.976	12.0		3
10.756	1.981	37.5		4
10.772	1.987	67.5	4.2	4
10.784	1.991	23.0		6
10.800	1.997	7.0		4
10.810	2.001	11.5	3.3	10
10.836	2.011	9.5	3.4	2
10.856	2.019	20.5	3.2	2
10.881	2.027	47.5	4.5	16
10.923	2.043	34.0		3
10.932	2.046	34.5		6
10.944	2.052	37.5	4.3	12
10.990	2.064	17.0	3.9	13
11.013	2.077	3.8		5

TABLE 1 (continued)

Frequency of peak - mc.	Energy of peak - Mev.	Amplitude of peak	Width at half max. - Kev.	Separation from next peak - Kev.
11.026	2.082	7.5		3
11.034	2.085	10.0		5
11.048	2.090	21.0		5
11.061	2.095	49.0	4.4	11
11.090	2.106	6.5		7
11.110	2.113	23.5	3.1	12
11.141	2.125	35.5	4.3	5
11.154	2.130	31.5		6
11.170	2.136	11.0		11
11.199	2.147	2.5		3
11.206	2.150	4.5	4.7	10
11.233	2.160	7.2		7
11.250	2.167	17.0	4.2	7
11.268	2.174	9.5	5.1	7
11.286	2.181	6.5		5
11.300	2.186	7.2		4
11.310	2.190	29.5	3.5	20
11.362	2.210	36.0	3.2	6
11.375	2.216	14.5		7
11.394	2.223	58.0	5.1	5
11.406	2.228	40.5		10

TABLE 1 (continued)

Frequency of peak - kc/s.	Energy of peak - 10^6	Amplitude of peak	Width at half max. - 10^6	Separation from max. peak - 10^6
11.026	2.022	9.5		3
11.034	2.085	10.0		2
11.046	2.090	21.0		1
11.061	2.095	49.0	4.4	11
11.070	2.106	6.5		7
11.130	2.113	25.5	3.1	12
11.141	2.125	15.5	4.3	3
11.154	2.130	31.5		6
11.170	2.130	11.0		14
11.199	2.147	2.5		3
11.206	2.150	4.5	4.7	10
11.233	2.160	7.2		7
11.250	2.167	17.0	4.2	7
11.264	2.174	9.5	3.1	7
11.284	2.181	6.5		5
11.300	2.188	7.0		4
11.310	2.190	29.5	3.5	10
11.328	2.210	36.0	3.2	8
11.375	2.216	14.5		7
11.394	2.217	36.0	3.3	5
11.406	2.222	40.5		10

TABLE 1 (continued)

Frequency of peak - mc.	Energy of peak - Mev.	Amplitude of peak	Width at half max. - Kev.	Separation from next peak - Kev.
11.433	2.238	40.0	4.4	12
11.464	2.250	10.0		7
11.482	2.257	31.0		4
11.491	2.261	70.5	4.4	6
11.506	2.267	13.5		12
11.537	2.279	20.5	5.5	9
11.559	2.288	34.0	3.4	5
11.572	2.293	6.0		6
11.586	2.299	11.0		3
11.595	2.302	19.0		5
11.608	2.307	26.5	4.6	7
11.624	2.314	23.0	2.5	6
11.639	2.320	10.0		5
11.652	2.325	34.5		5
11.665	2.330	28.5		11
11.692	2.341	4.5		3
11.700	2.344	4.0		6
11.715	2.350	10.5	4.3	4
11.726	2.354	5.0		4
11.734	2.358	6.0		4
11.745	2.362	8.5	4.8	5

TABLE I (continued)

Frequency MC/sec - mc	Period of Wave - sec	Amplitude of Wave	Width at Half max. - km	Duration (Cycle Half Wave - sec)
11.433	2.230	40.5	44.4	12
11.444	2.230	10.0		7
11.455	2.227	31.0		4
11.493	2.221	76.5	44.4	6
11.506	2.217	13.5		12
11.537	2.212	20.5	34.3	9
11.559	2.208	16.0	34.4	3
11.572	2.203	6.0		6
11.585	2.199	11.0		3
11.595	2.203	19.0		3
11.602	2.207	20.5	44.8	7
11.622	2.214	23.0	34.2	6
11.639	2.220	10.0		3
11.672	2.232	34.5		8
11.685	2.239	32.5		12
11.694	2.241	4.5		3
11.709	2.244	4.0		4
11.712	2.250	10.5	44.3	4
11.720	2.254	5.0		4
11.734	2.260	6.0		4
11.745	2.265	6.5	44.2	3

TABLE 1 (continued)

Frequency of peak - mc.	Energy of peak - Mev.	Amplitude of peak	Width at half max. - Kev.	Separation from next peak - Kev.
11.757	2.367	9.5	2.8	5
11.770	2.372	14.5		3
11.777	2.375	32.0		3
11.785	2.378	27.5		2
11.789	2.380	26.0		4
11.800	2.384	25.5		4
11.810	2.388	11.5		3
11.817	2.391	8.0		4
11.827	2.395	16.5		6
11.841	2.401	26.0		7
11.859	2.408	10.0		4
11.868	2.412	22.5	3.0	5
11.880	2.417	10.0		5
11.892	2.422	9.0		4
11.902	2.426	8.5		2
11.908	2.428	5.0		8
11.926	2.436	45.5	3.8	9
11.950	2.445	33.0	3.9	6
11.963	2.451	10.5		5
11.976	2.456	20.5	3.5	7

TABLE 1 (continued)

Measurement of depth - cm.	Number of depth - [illegible]	Deviations of mean - [illegible]	Yields as built mean - [illegible]	Measurements from mean - [illegible]
12.750	2.307	3.3	0.3	3
12.770	2.193	14.3		3
12.777	4.193	34.3		3
12.780	3.378	47.3		3
12.785	2.388	36.0		4
12.800	2.384	53.3		4
12.810	3.378	11.3		3
12.817	3.393	8.0		4
12.827	3.393	14.3		4
12.841	3.411	26.0		7
12.859	2.578	13.0		4
12.860	3.434	33.3	3.0	5
12.880	3.437	20.0		5
12.892	2.420	3.0		4
12.900	3.428	8.3		4
12.908	3.422	3.7		3
12.920	3.438	45.3	3.3	8
12.930	3.445	73.0	3.7	6
12.953	3.423	10.3		3
12.978	3.438	50.3	3.3	7

TABLE 1 (continued)

Frequency of peak - mc.	Energy of peak - Mev.	Amplitude of peak	Width at half max. - Kev.	Separation from next peak - Kev.
11.992	2.463	28.0		5
12.004	2.468	31.5		13
12.038	2.481	40.0	3.3	10
12.061	2.491	10.5		5
12.072	2.496	38.5	3.3	3
12.080	2.499	19.0		9
12.102	2.508	57.0	3.8	-

TABLE 2 (CONTINUED)

Percentage of Spark - 3%	Energy at Peak - Joules	Duration of Spark	Ratio of Spark Duration to Peak - 10%	Indicating Time Spark - 10%
12.992	2.163	20.0		5
12.001	2.164	22.5		13
12.038	2.163	40.0	3.2	10
12.021	2.164	20.5		5
12.093	2.156	22.5	3.2	7
12.050	2.159	25.0		5
12.107	2.158	27.0	3.0	-

$$\text{Mass Difference}^{4}\ (Ti^{45} - Sc^{45}) = -Q - (n-p)$$
$$= (0.003061 \pm 0.000003) - (0.000840 \pm 0.000005) \quad (B3)$$
$$= 0.002221 \pm 0.000006 \text{ amu}$$

The background was not measured over the energy range covered, because of changes made on the generator before this could be done. However, the background in the region of 2.5 Mev was measured, and was substantially the same as the yield obtained below threshold. The experimental points are shown by circles. The magnitude of the probable error in these points is indicated along the axis of ordinates. The experimental points are connected by straight lines, for reasons discussed below.

Table 2 lists all of the peaks in the neutron yield. The narrowest peak found, at 2.929 Mev had a width of 5 Kev at half its maximum amplitude. This sets an upper limit of 5 Kev to the target thickness. The resolution of the peaks was not considered good enough to justify fairing in a smooth curve through the experimental points. Therefore, the points were connected by straight lines to avoid obscuring any details. It is believed that better resolution could be obtained by the use of a thinner target, as in the chlorine experiment.

---

4. See footnote 2 on page 18.

Mass difference[4] $|\Delta\Omega^{5} - \Omega_{\Delta}^{5}| = m - 0 - (n-p)$

$$= (0.00391 \pm 0.00007) - (0.00840 \pm 0.00002) \qquad (23)$$

$$= 0.00223 \pm 0.00006 \text{ mu}$$

The background was not measured over the energy range covered, because of changes made on the generator before this could be done. However, the background in the region of 5.5 Mev was measured, and was substantially the same as the yield obtained below threshold. The experimental points are shown by circles. The magnitude of the probable error in these points is indicated along the axis of ordinates. The experimental points are connected by straight lines, for reasons discussed below.

Table 2 lists all of the peaks in the neutron yield. The narrowest peak found, at 3.999 Mev had a width of 5 Kev at half its maximum amplitude. This sets an upper limit of 5 Kev to the target thickness. The resolution of the peaks was not considered good enough to justify fitting in a smooth curve through the experimental points. Therefore, the points were connected by straight lines to avoid obscuring any details. It is believed that better resolution could be obtained by the use of a thinner target, as in the calcium experiment.

---

4. See footnote 2 on page 16.

TABLE 2
RESONANCE PEAKS IN NEUTRON YIELD FROM $Sc^{45}(p,n)Ti^{45}$
Error in E ± 0.1%, relative to $Li^{7}(p,n)$ threshold

Frequency of peak - mc.	Energy of peak - Mev.	Amplitude of peak	Width at half max. - Kev.	Separation from next peak - Kev.
13.050	2.916	6.4		4
13.059	2.920	7.5		9
13.078	2.929	8.0	4.6	8
13.096	2.937	7.8	5.7	9
13.116	2.946	7.6		2
13.122	2.948	7.1		11
13.146	2.959	7.7		5
13.159	2.964	19.0	5.5	9
13.176	2.973	10.1		5
13.188	2.978	12.0	5.2	5
13.198	2.983	11.2		5
13.210	2.988	12.8		4
13.218	2.992	10.8		4
13.228	2.996	13.0		8
13.246	3.004	9.2		6
13.259	3.010	9.8		6
13.272	3.016	10.3		3
13.279	3.019	18.4	6.6	8
13.295	3.027	11.7		7
13.310	3.034	14.5		5

TABLE 2

SUPERLUMINAL PEAKS IN RECEDING VIEWING SPACE OF $L^{45}(p,n)T^{45}$ STARTING IN 2 ± 0.1%, RELATIVE TO $L^{9}(p,n)$ STANDARD

Frequency of peak - (Mc)	Energy of peak - (keV)	Amplitude of peak	Width at half max. - (keV)	Separation from main peak - (keV)
13.030	3.918	6.4		6
13.037	3.920	9.5		9
13.043	3.922	6.0	4.6	6
13.050	3.937	9.8	5.9	9
13.116	3.946	9.0		2
13.123	3.948	9.1		11
13.129	3.959	9.7		5
13.139	3.964	19.0	5.5	9
13.176	3.973	10.1		5
13.183	3.974	13.0	5.3	5
13.190	3.983	11.2		2
13.230	3.994	12.8		4
13.236	3.994	10.6		4
13.243	3.996	13.0		2
13.249	3.998	9.2		6
13.279	3.010	9.8		8
13.273	3.013	10.3		3
13.279	3.019	13.1	6.6	8
13.293	3.027	11.7		7
13.320	3.034	18.3		5

TABLE 2 (continued)

Frequency of peak - mc.	Energy of peak - Mev.	Amplitude of peak	Width at half max. - Kev.	Separation from next peak - Kev.
13.322	3.039	12.6		5
13.332	3.044	13.4		7
13.348	3.051	11.9		4
13.358	3.055	12.2		6
13.370	3.061	14.7		3
13.378	3.064	19.3		6
13.390	3.070	16.0		7
13.404	3.077	13.5		7
13.420	3.084	14.0		8
13.438	3.092	15.3		5
13.448	3.097	13.5		6
13.462	3.103	15.6		3
13.468	3.106	18.8		3
13.478	3.109	15.0		11
13.498	3.120	14.6		5
13.508	3.125	14.0		-

TABLE 6 (continued)

Frequency of peak - cps.	Energy of peak - db.	Amplitude of peak	Width at half max. - db.	Separation from next peak - cps.
13.322	3.039	12.6		5
13.334	3.024	17.4		7
13.340	3.023	11.7		4
13.350	3.032	10.3		6
13.370	3.041	14.7		3
13.378	3.054	19.3		6
13.398	3.070	16.0		7
13.404	3.097	13.3		7
13.420	3.104	14.0		8
13.428	3.092	15.3		9
13.444	3.094	13.3		6
13.463	3.109	17.8		3
13.468	3.106	14.8		3
13.479	3.109	19.0		11
13.498	3.130	16.6		2
13.506	3.139	14.0		-

General: The yield of neutrons was measured throughout, not as counts per second, but as counts per micro coulomb of the proton beam as determined from a beam current integrator. In this way the counting rate was normalized against any fluctuations in the beam current. Since no correction was made to the counting rate for the efficiency of the long counter, the yield will be distorted at low neutron energies just above the threshold.

The maximum counting rate obtained during either experiment was 14,000 counts per 200 micro coulombs. This corresponds to 3 micro amperes striking the target for 67 seconds. Thus the maximum counting rate was less than 250 counts per second, with an average time between pulses of more than 4,000 micro seconds. The scaler had a resolving time of 5 micro seconds, the amplifier a rise time of 0.5 micro seconds and a clipping time of 2 micro seconds. Since these times were very much less than 4,000 micro seconds, no corrections were necessary in the counting rates.

Figures 5 and 6 show the reproducibility of several peaks, with measurements taken at different times. In order to insure that there had been no appreciable change in target thickness, build up of surface contaminants, or changes in the overall operation of the measuring equipment due to unknown causes, the same peak was measured at

Counts: The yield of neutrons was measured throughout, and as counts per second, not as counts per minute one-half of the proton beam as determined from a beam current integrator. In this way the counting rate was unaffected against any fluctuations in the beam current. Since no correction was made to the counting rate for the efficiency of the long counter, the yield will be distorted at low neutron energies just above the threshold.

The maximum counting rate obtained during either period was 14,000 counts per 100 micro coulombs. This corresponds to 3 micro ampere striking the target for 67 seconds. Thus the maximum counting rate was less than 250 counts per second, with an average time between pulses of more than 4,000 micro seconds. The scaler had a resolving time of 3 micro seconds, the amplifier a rise time of 0.5 micro seconds and a slippage time of 2 micro seconds. Thus these times were very much less than 4,000 micro seconds, so corrections were necessary in the counting rates.

Figures 5 and 6 show the cross-probability of several peaks, with measurements taken at different times. In order to insure that there had been no appreciable change in target thickness, build up of surface contaminants, or changes in the overall operation of the measuring equipment due to various causes, the same peak was measured at

Figure 5

REPRODUCIBILITY OF PEAKS

$Cl^{37}(p,n)A^{37}$

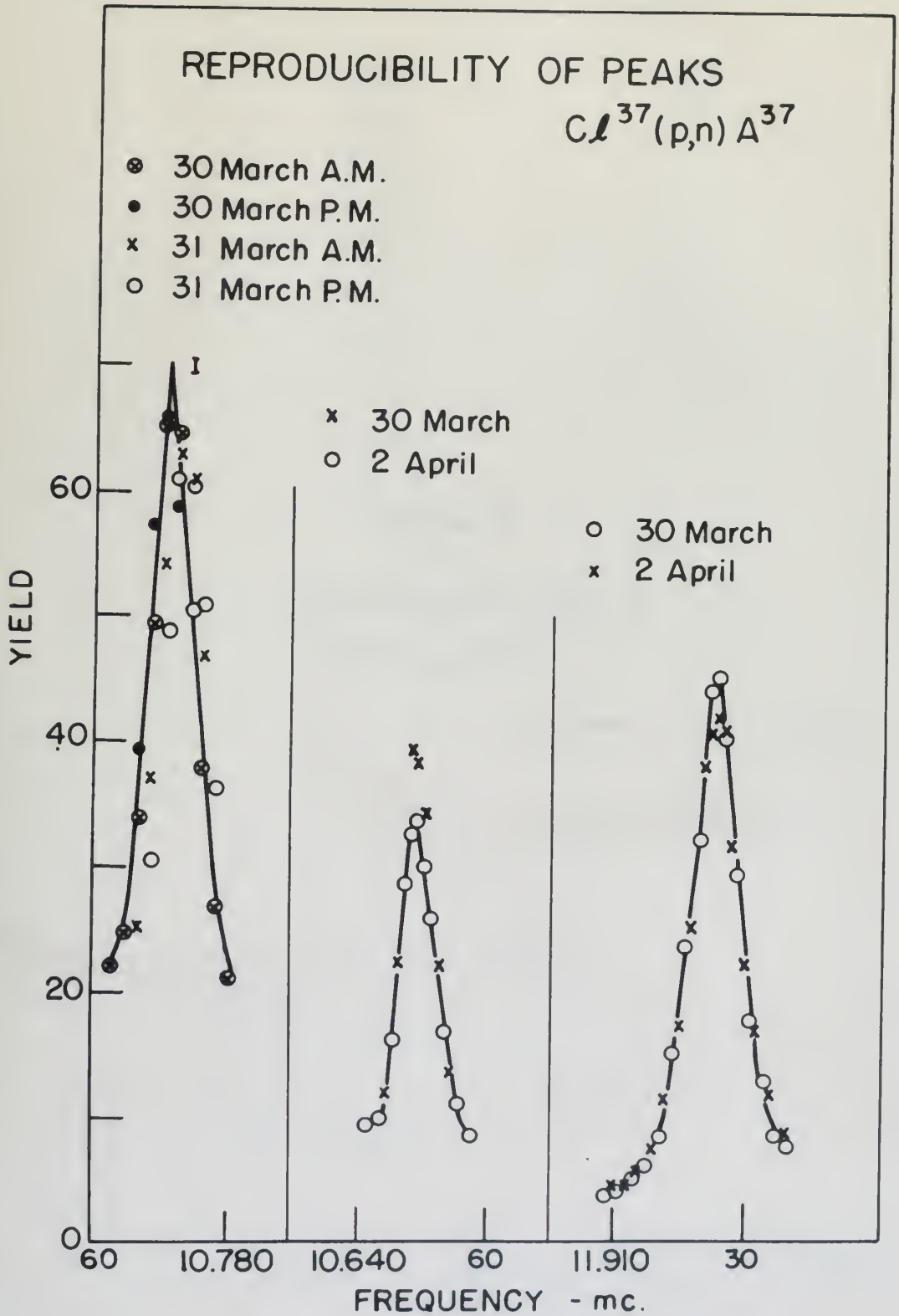
REPRODUCIBILITY OF PEAKS
Cl37(p,n) A37
30 March A.M.
30 March P.M.
31 March A.M.
31 March P.M.
30 March
2 April
30 March
2 April
YIELD
0
20
40
60
60
10.780
10.640
60
11.910
30
FREQUENCY - mc.

Figure 6

REPRODUCIBILITY DATA

$Sc^{45}(p,n)Ti^{45}$

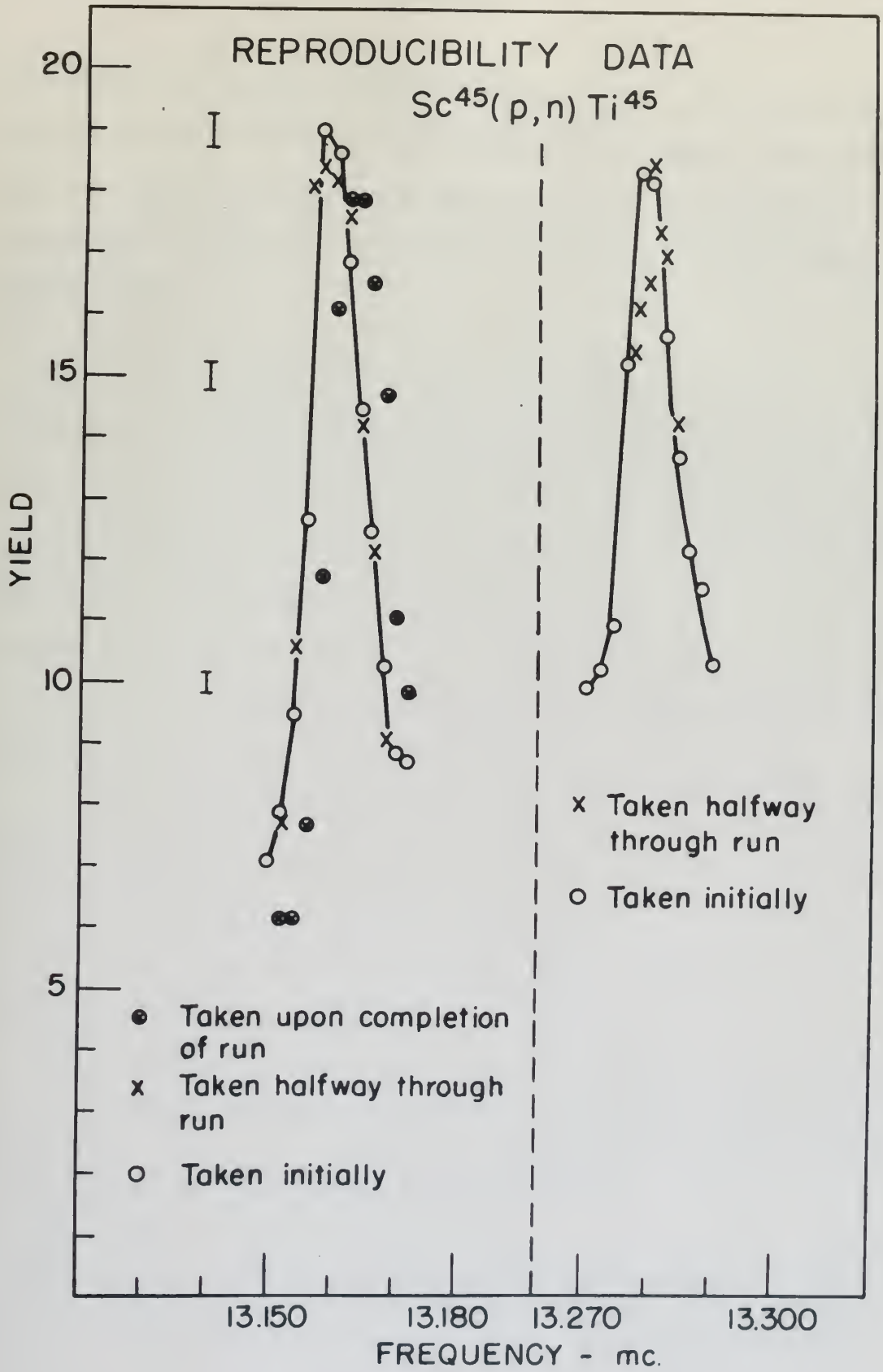
REPRODUCIBILITY DATA
$Sc^{45}(p,n)Ti^{45}$
YIELD
20
15
10
5
13.150
13.180
13.270
13.300
FREQUENCY - mc.
Taken upon completion of run
x Taken halfway through run
o Taken initially
x Taken halfway through run
o Taken initially

the start and finish of each separate run. It can be seen that the amplitudes and positions of the maxima vary slightly, but the variation in position is much less than the 0.1% mentioned on page 8. The target thickness did not change appreciably.

the start and finish of each separate run. It can be seen that the amplitudes and positions of the maxima vary slightly, but the variation in position is much less than the 0.1% mentioned on page 8. The target thickness did not change appreciably.

CHAPTER V

THEORETICAL CONSIDERATIONS

Neutron Energies: The neutron yield from the $Li^7(p,n)Be^7$ reaction is often used as a neutron source. However, there are two disadvantages to the use of these neutrons in some experiments. The lowest energy neutrons obtainable, in the forward direction, just at the threshold, are 29 Kev. In addition, there is a large variation of neutron energy with angle of emission in the laboratory coordinates. For example, at a proton energy of 2.0 Mev, the neutron energy at 0° is 228 Kev, while the energy at 180° is 15 Kev. Willard (W1) tabulates the neutron energies at different angles for a wide range of proton energies.

Since both of these effects are caused by the motion of the compound nucleus, a heavier target nucleus would provide lower energy neutrons in the forward direction at the threshold, and also less variation in neutron energy with angle at all energies.

The following expression for the energy of the neutrons from the $Sc^{45}(p,n)Ti^{45}$ reaction is derived from the laws of conservation of mass-energy and momentum:

$$E_n^{\frac{1}{2}} = \frac{E_p^{\frac{1}{2}}}{46} \cos\theta \pm \left[\left(\frac{44}{46} + \frac{\cos^2\theta}{(46)^2}\right) E_p + \frac{45}{46} Q\right]^{\frac{1}{2}}$$

CHAPTER V

KINEMATICAL CONSIDERATIONS

Neutron Energies: The neutrons yield from the $Li^7(p,n)Be^7$ reaction is often used as a neutron source. However, there are two disadvantages to the use of these reactions in some experiments. The lowest energy neutrons obtainable, in the forward direction, just at the threshold, are 29 kev. In addition, there is a large variation of neutron energy with angle of emission in the laboratory coordinates. For example, at a proton energy of 2.0 mev, the neutron energy at 0° is 322 kev, while the energy at 180° is 15 kev. Willard (31) tabulates the neutron energies at different angles for a wide range of proton energies.

Since both of these effects are caused by the motion of the compound nucleus, a heavier target nucleus would provide lower energy neutrons in the forward direction at the threshold, and also less variation in neutron energy with angle at all energies.

The following expression for the energy of the neutrons from the $Be^9(p,n)B^9$ reaction is derived from the laws of conservation of mass-energy and momentum:

$$E_n^{\frac{1}{2}} = \frac{E_p^{\frac{1}{2}}}{A_0} \cos\theta \pm \left[\left(\frac{A_1}{A_0} + \frac{\cos^2\theta}{(A_0)^2}\right) E_p + \frac{A_2}{A_0}\right]^{\frac{1}{2}}$$

E_n = neutron energy in Kev.

E_p = proton energy in Kev.

θ = angle of emission of neutrons with respect to direction of incident proton, in laboratory coordinates.

Q = -2850 Kev (see page 23).

From this expression, the energy of the neutrons emerging at threshold (E_p = 2.913 Mev), (θ = 0), is 1.4 Kev. One of the largest neutron yields was obtained with a proton energy of 2.964 Mev. The energy of these neutrons at various angles is given below:

θ	0°	90°	180°
E_n	67.8 Kev	53.4 Kev	34.5 Kev

Thus, it is seen that neutrons from scandium can be obtained at energies as low as 1.4 Kev, compared to the minimum energy of 29 Kev from lithium. For any given energy, neutrons are available from scandium which have less variation in energy with angle than those obtained from lithium. Since the absolute yield of neutrons from scandium was not determined in this experiment, it is not known whether this reaction could be used as a neutron source in work requiring a high flux.

Taschek and Hemmendinger (T2) measured the absolute yield of the $Li^7(p,n)Be^7$ reaction. This required a know-

E_n = neutron energy in Mev.

E_p = proton energy in Mev.

θ = angle of emission of neutrons with respect to direction of incident protons, in laboratory coordinates.

Q = -2.226 Mev (see page 23).

From this expression, the energy of the neutrons emerging at threshold (E_p = 2.223 Mev), (θ = 0), is 1.4 Mev. One of the largest neutron yields was obtained with a proton energy of 2.324 Mev. The energy of these neutrons at various angles is given below:

θ	0°	30°	120°
E_n	87.5 Mev	33.4 Mev	14.3 Mev

Thus, it is seen that neutrons from reaction can be obtained at energies as low as 1.4 Mev, compared to the minimum energy of 29 Mev from lithium. For any given energy, neutrons are available from reaction which have less variation in energy with angle than those obtained from lithium. Since the absolute yield of neutrons from reaction was not determined in this experiment, it is not known whether this reaction could be used as a neutron source in work requiring a high flux.

Jaeckel and Trumbulloge (23) measured the absolute yield of the $Li^7(p,n)Be^7$ reaction. This required a knowe-

ledge of the actual target thickness, which was obtained from the "geometric peak." Since scandium is heavier, it is impractical to measure the "geometric peak," and the target thickness must be determined by other means. The upper limit to the target thickness, discussed previously, includes the actual target thickness, the spread in energy of the protons, and the actual width of the energy level.

If one of the peaks were remeasured using a much thinner target, and had a considerably narrower width, then the actual target thickness of the original target would be known to within the width of the thinner target. Thus, if the thicker target had a peak of 5 Kev width, and this peak, when remeasured with a thinner target, had a width of 1 Kev, then the original target thickness would be 5 ± 1 Kev.

A determination of the yield relative to lithium also requires a knowledge of the actual target thickness. However, it is estimated that the neutron yield from scandium is many times less than that obtained from lithium. This estimate is based on an experimental knowledge of the counting rates from the two reactions for different counter geometries.

<u>Energy Levels</u>: In the p,n reaction, a proton of angular momentum $\bar{\ell}$, and spin $\bar{i} = \frac{1}{2}$, bombards a target nucleus of spin $\bar{I}$. The vector channel spin $\bar{s} = \bar{i} + \bar{I}$ combines with the vector angular momentum of the proton ℓ,

ledge of the normal target thickness, which was obtained from the "geometric peak." Since resolution is nearly, it is impossible to measure the "geometric peak," and the target thickness must be determined by other means. The upper limit to the target thickness, discussed previously, includes the normal energy thickness, the spread in energy of the neutrons, and the natural width of the energy level.

If one of the peaks were measured using a much thinner target, and had a considerably smaller width, then the actual target thickness of the original target would be known to within the width of the thinner target. Thus, if the thinner target had a peak of 2 Mev width, and this peak, when remeasured with a thicker target, had a width of 1 Mev, then the original target thickness would be 2 ± 1 Mev.

A determination of the yield relative to fission also requires a knowledge of the normal target thickness. However, it is estimated that the neutron yield from resonance is many times less than that obtained from fission. This estimate is based on an approximate knowledge of the cross-section from the two measures for different neutron energies.

General Theory: In the p,n reaction, a proton of angular momentum $\vec{j}$, and spin $\vec{I} = \frac{1}{2}$, bombards a target nucleus of spin $\vec{I}$. The recoil nucleus spin $\vec{J} = \vec{I} + \vec{j}$ combines with the recoil angular momentum of the proton $\vec{j}$,

to give the spin $\bar{J} = \bar{s} + \bar{\ell}$ of the compound nucleus. Since a proton has an intrinsic even parity, compound nuclei formed from even values of ℓ, will have the same parity as the target nucleus; whereas those formed from odd values of ℓ will have the opposite parity. Mathematically, off-center collisions ($\ell > 0$) can be treated in terms of dead-center collisions, ($\ell = 0$), by adding a fictitious "centrifugal barrier" term which increases rapidly with ℓ. For the energies used in this experiment, it was assumed that the "centrifugal barrier" for $\ell > 1$ was so large that the probability of forming the compound nucleus was small. Thus, ℓ can have the values of 0 or 1. The laws of quantum mechanics permit the following values of J:

For $\ell = 0$; $J = s = I - \frac{1}{2}$ or $I + \frac{1}{2}$, same parity as target.

For $\ell = 1$; $s = I - \frac{1}{2}$, $J = I - 3/2$, $I - \frac{1}{2}$, or $I + \frac{1}{2}$

$s = I + \frac{1}{2}$, $J = I - 1/2$, $I + \frac{1}{2}$, or $I + 3/2$ opposite parity as target.

Non-identical quantum states of the compound nucleus correspond to different energy levels. If the states having the same value of J and ℓ, but different s, are not identical, there will be a separate energy level for each of the eight combinations shown above. If they are identical, these eight combinations result in six different energy levels.

To give the zeta $\bar{z} = \bar{x} + \bar{i}$ of the corresponding matrix, there
a system has an infinite area quality, suggested physical
theory from zero values of λ, will have the more priority
to the typical instance; whereas lower lowed from not values
of λ will have the opposite quality. Mathematically, off-
center collisions ($\lambda > 0$) can be treated in terms of cen-
tral collisions. ($\lambda = 0$), by adding a fictitious repulsi-
ve "barrier" term which increases rapidly with λ. The
the molecule used in this calculation, it was assumed that
the "geometrical barrier" for $\lambda > 1$ was so large that the
probability of leaving the excited molecule was small. Thus,
λ can have the values of 0 or 1. The laws of quantum me-
chanics permit the following values of λ:

For $\lambda = 0$: $\lambda = x = i - \frac{1}{2}$ or $i + \frac{1}{2}$, which permit no
change.

For $\lambda = 1$: $x = i - \frac{1}{2}$, $i + 1/2$, $i - \frac{1}{2}$, or $i + \frac{1}{2}$

$x = i + \frac{1}{2}$, $i + 1/2$, $i + \frac{1}{2}$, or $i + 1/2$
permitting no change.

Non-integral quantum states of the suggested molecule
correspond to different energy levels. If the atoms having
the same value of i and λ, but different x, are not identi-
cal, there will be a separate energy level for each of the
eight wavefunctions given above. If they are identical, there
eight wavefunctions result in six different energy levels.

By analogy with spectroscopy, these six or eight related energy states are considered a multiplet, and exist for a given total quantum number. This total quantum number is not defined, but is assumed to be analogous with the orbital quantum number n in atomic theory. From this, it is expected that the multiplet would be repeated as n takes on different values.

On a single particle model of the nucleus, it could be supposed that, just before the emission of a neutron, the compound nucleus could be represented by a wave function describing the neutron moving in the force field of the residual nucleus. This wave function would be characterized by the excitation energy and the coupling of the angular momentum, ℓ , and the spin, i, of the neutron with the residual nucleus. As the p,n reaction is a reversible process, the compound nucleus must have values of J which can be formed not only from a proton and the target, but also from a neutron and the residual nucleus. If the spin of the residual nucleus were known, the other half of the problem could be worked out, and those values of J common to both would be the ones actually observed. However, both of the residual nuclei of this experiment, A^{37} and Ti^{45}, have unknown spins, so that the complete problem cannot be worked out.

If the spacing of the states of a multiplet were small

In analogy with spectroscopy, there are six or eight relative energy states are considered a multiplet, and which has a given total angular momentum. This total angular momentum is not defined, but is assumed to be associated with the spin, and quantum number s in nuclear theory. From this, it is suggested that the multiplet would be regarded as a taken as different orbits.

On a simple particle model of the nucleus, it could be suggested that, just before the scattering of a neutron, the compound nucleus could be represented by a very theoretically determining the maximum energy in the lower field of the transmuted nucleus. This more transition could be characterized by the statistical energy and the complexity of the angular momentum, δ , and the spin, I, of the neutron with the theoretical nucleus. In the $D_{3/2}$ resonance in a potassium isotope, the compound nucleus must have values of I which can be formed not only from a proton and the target, but also from a neutron and the residual nucleus. If the spin of the residual nucleus were known, the upper limit of the possible spin be reached and, and hence values of I common to both would be the same certainly determined. However, with of the residual nucleus of high uncertainty, I_{39} and I_{41}, have unknown spins, or that the compound nucleus cannot be reached yet.

If the spinless of the nucleus of a multiplet were small

compared with the spacing between multiplets, groups of six or eight resonance levels might be observed. However, there is a very good chance that states of different multiplets overlap, and also that the single particle picture may not be valid. Preston (P3) discusses the theory of the p,n reaction in detail.

The Sc^{45} nucleus has a spin of 7/2 so that the possible J values of the compound nucleus, Ti^{46}, would be 3 or 4, same parity, and 2, 3, 4, 3, 4, 5, opposite parity. From Figure 4, it can be seen that four of the peaks, at 2964, 3019, 3064, and 3106 Kev, are much larger than any of the other peaks. Also, each of these large peaks has a smaller peak just above it, and a much smaller peak, or an indication of one, just below it. This repeating triplet might indicate that each of the large peaks corresponds to a particular J value being repeated for different total quantum numbers. Between the first two large peaks, there are nine other peaks; between the next two, there are seven; and between the last two, six. The large peaks are occuring closer together at the higher energies, indicating that the multiplet spacing is decreasing. Thus, the observed number of peaks, twenty-five, if assigned to three multiplets, agrees very closely with the theoretical value of eight per multiplet. Table 3 shows the average energy level spacing of

compared with the playing between individuals, groups of six or eight randomness levels might be observed. However, there is a very good reason such values of difference mathematically, and also that the single particle pairing may not be valid. Theorem (29) strengthens the theory of the P.D expectation in detail.

The 49[45] sequence has a sum of 9/2 so that the possible 7 values of the compound scalars, r_{49}[46], would be 2 or 4, some parity, non 6, 2, 0, 2, 4, 6, opposite parity. From Figure 6, it can be seen that four of the pairs, at least, 2223, 3003, and 3206 Rev, are much larger than any of the other pairs. Also, each of these large pairs has a multiple pair that shows it, and a much smaller pair, or no indication of one, just below it. This responding helpful might indicate that pairs of the large pairs correspond to a particular 7 value being responsible for different total pairs two numbers. Between the right two large pairs, there are also other pairs; between the next two, there are one missing and between the last two, nine. The large pairs are showing almost temporary at the bigger separation, indicating that the multiple pairing is decreasing. Thus, the observed number of pairs, twenty-five, if assigned to three individuals, appears very closely with the theoretical value of eight for multiplet. Table 3 shows the average number level spacing of

TABLE 3
SPACINGS IN Ti^{46}

Energy of peak at start of interval-Mev.	Energy of peak at end of interval-Mev.	Energy between peaks Kev.	Levels between peaks	Average level spacing
2.964	3.019	55	9	5.5
3.019	3.064	45	7	5.6
3.064	3.106	42	6	6.0
2.964	3.106	142	24	5.7
2.916	3.125	209	34	6.0

TABLE 3.44

[illegible]

Energy of peak at start of interval-keV	Energy of peak of end of interval-keV	Number between peaks-Cnt.	Levels between peaks	Level spacing
2.764	3.019	55	9	3.3
3.019	3.064	43	7	3.4
3.064	3.106	42	6	4.0
3.106	3.126	149	24	3.7
3.126	3.175	209	34	4.0

Ti^{46}, as observed from the yield curve (Figure 4).

The Cl^{37} nucleus has a spin of 3/2, so that the possible values of J of the compound nucleus, A^{38}, would be 1 or 2, same parity, and 0, 1, 2, 1, 2, or 3, opposite parity. The yield curve (Figure 2) was examined in an attempt to find a similar repeating pattern. Although there were many large peaks, none of them were conspicuously different from the remainder, as was the case in scandium. A number of possible repeating patterns could be picked out from among all of the available peaks. One scheme, using a triplet similar to the one in scandium, gave 128 peaks in 14 multiplets. This doesn't agree with the theoretical value too well, but it is fairly close. Table 4 shows the average energy level spacing of A^{38} based on this scheme. The intervals were taken between the large center peaks of the triplets.

The proton energy for a peak in the yield curve is known to an accuracy of 0.1%, relative to the measured value of the Li^{7}(p,n) threshold, as previously discussed. If these energies were corrected for motion of the center of mass, loss of energy in the target, and displacement of the peak due to the effect of neighboring peaks, the energy levels of the compound nuclei can be obtained by adding the proton binding energy to the corrected proton kinetic energies. The average energy level spacing obtained from the

72^{66}, as observed from the yield curve (Figure 4).

The G_{77} resonance has a width of $1/2$, so that the position values of 1 of the compound analogs, A^{77}, would be 1 or 2, some partly, and 0, 1, 2, 3, 4, or 5, appreciable amounts. The yield curve (Figure 4) was constructed in an attempt to find a similar expanding pattern. Although there were many large peaks, none of them were significantly different from the remainder, as was the case in neutrons. A number of possible expanding patterns could be plotted out from among all of the available peaks. One attempt, using a triple ellipse by the one in neutrons, gave 120 peaks in 12 ellipses. This doesn't agree with the theoretical value for well, but it is fairly close. Table 4 shows the average energy level spacing of $1/2^{+}$ based on this scheme. The low energies were taken between the large energy peaks of the triplets.

The proton energy for a peak in the yield curve is known to an accuracy of 0.12, relative to the measured value of the 12 (p,n) groundstate, as previously discussed. If these energies were corrected for masses of the center of mass, loss of energy to the target, and displacement of the peak due to the effect of neutrons leaving, the energy levels of the compound nucleus can be obtained by adding the proton binding energy to the corrected proton kinetic energies. The average energy level spacing obtained from the

differences in the energies of the peaks in the yield curves will be accurate, since these corrections will cancel out.

TABLE 4

SPACINGS IN A^{38}

Energy of peak at start of interval-Mev.	Energy of peak at end of interval-Mev.	Energy between peaks Kev.	Levels between peaks	Average level spacing
1.691	1.773	82	10	7.5
1.773	1.819	46	7	5.8
1.819	1.851	32	6	4.6
1.851	1.892	41	8	4.6
1.892	1.942	50	10	4.5
1.942	1.987	45	7	5.6
1.987	2.046	59	7	7.4
2.046	2.095	49	6	7.0
2.095	2.167	72	8	8.0
2.167	2.261	94	11	7.8
2.261	2.325	64	9	6.4
2.325	2.375	50	9	5.0
2.375	2.412	37	8	4.1
2.412	2.463	51	8	5.7
1.691	2.463	772	127	6.0
1.644	2.508	864	140	6.1

TABLE 4

SUCCESS VS. D_{34}

Number of jobs by which of industrial-ists.	Number of jobs at and of industrial-ists.	Number be-ween jobs D_{34}.	Invalid Level Tests Invalid	Invalid Level Tests Valid
1.002	1.773	23	16	7.3
1.773	1.219	46	9	3.2
1.019	1.021	32	6	5.8
1.021	1.320	41	8	4.0
1.022	1.343	32	31	1.3
1.341	1.577	43	9	3.6
1.577	2.010	29	7	7.6
2.010	2.023	49	6	7.0
2.023	2.347	73	4	1.9
2.127	2.321	34	15	7.6
2.321	2.325	44	9	4.9
2.323	2.375	32	4	7.0
2.375	2.413	37	8	4.1
2.413	2.403	31	4	3.7
1.031	2.413	773	127	6.0
1.044	2.320	344	120	4.1

BIBLIOGRAPHY

B1 Baker, Howell, Goodman, and Preston, P.R. 81, 48 (1951)

B2 Baker and Howell, M.I.T. Thesis, June, 1950

B3 Bainbridge, P.R. 81, 146L (1951)

E1 Elmore and Sands, "Electronics Experimental Techniques," National Nuclear Energy Series V-1, McGraw Hill, First Edition, 1949, Chapter 3

H1 Herb, P.R. 75, 246 (1949)

H2 Herb, P.R. 76, 502 (1949)

H3 Hadden, M.I.T. Thesis, December, 1950

H4 Hanson and McKibben, P.R. 72, 673 (1947)

J1 Jennings, Proc. of the I.R.E. Vol. 38 N, October 10,1950

M1 McCue and Preston, P.R. 81, 318A (1951)

P1 Preston and Stelson, private communication

P2 Preston, "The Reduction of the Proton Resonance Frequency Scale to an Energy Scale," unpublished

P3 Preston,"The p,n reaction," unpublished

R1 Richards, Smith and Browne, P.R. 80, 524 (1950)

T1 Taschek, unpublished

T2 Taschek and Hemmendinger, P.R. 74, 373 (1948)

BIBLIOGRAPHY

[1] Baker, Donald, Bookman, and Freedman, P.M. 42, 40 (1951)

[2] Baker and Donald, N.I.H. Bombay, Jaipur, 1950

[3] Gainsbrugh, P.M. 23, 1466 (1952)

[4] Alpers and Gomez, "Experience in Decentralized Production," National Industrial Survey Series No1, Bombay 1111, Times Building, 1950, Chapter 3

[5] Lewis, P.M. 22, 246 (1949)

[6] Lewis, P.M. 22, 302 (1949)

[7] Gadkari, N.I.H. Jaipur, December, 1950

[8] Gossen and Jenicoms, P.M. 22, 87) (1947)

[9] Tomalin, Index of the N.I.H. Vol. 30 N, October 4,1950

[10] Bodine and Orphicon, P.M. 23, 1181 (1951)

[11] Trewin and Shallcon, private communication

[12] Trewin, "The Solution of Non Linear Problems Involving Depth Data to an Energy Level," unpublished

[13] Trewin, "The N.M Problem," unpublished

[14] Kirkwood, Bull. Soc Chemie, T.P. 30, 256 (1950)

[15] Kirkwood, unpublished

[16] Tomalin and Bannerjiwar, P.M. 24, 203 (1948)

BIBLIOGRAPHY (continued)

W1 Willard, Preston, and Goodman, O.N.R. Technical Report No. 45, September, 1950

W2 White, P.R. 56, 512 (1939)

W3 White, P.R. 59, 63 (1941)

ACKNOWLEDGMENTS

The graduate study of Lieutenant Commander William A. Schoenfeld and Lieutenant Commander Robert W. Duborg at M.I.T. was sponsored by the United States Naval Postgraduate School and the Bureau of Ordnance, Navy Department. The work herein reported was undertaken under the Nuclear Shielding Project at M.I.T., which is sponsored by the Bureau of Ships and the Office of Naval Research.

The authors desire to express their deep appreciation to Dr. Clark Goodman for his guidance as thesis supervisor; and to Drs. W.M. Preston, J.J. McCue, P.H. Stelson, Messrs. D.C. Thompson, and I.E. Slawson, and the many personnel of the Laboratory for Nuclear Science and Engineering who were so generous with their aid in conducting experiments at the Rockefeller generator.

ACKNOWLEDGEMENTS

The grateful acknowledgements are due to the Commonwealth Mining and Metallurgical Research Laboratories, Department of Mines, Perth, for financial assistance during the period of this research. The work herein described was undertaken under the Australian Metals Research Council Project 4.4.7, which is sponsored by the Bureau of Mines and the Office of Naval Research.

The author wishes to express their deep appreciation to Dr. Clark Goodman for his guidance as thesis supervisor; and to Drs. E.H. Frankis, J.J. Moore, T.G. Nelson, Messrs. L.E. Thompson, and L.E. Clemens, and the entire personnel of the Laboratory for Metallurgical Science and Technology who were so generous with their aid in conducting experiments at the Metallurgical Laboratory.

Thesis
S34
15655

Schoenfeld

Energy levels in A38 and Ti46 from the p,n reaction on Cl37 and Sc45 respectively

Date Due

thesS34
Energy levels in A Superscript 38 and T
3 2768 002 00016 8
DUDLEY KNOX LIBRARY